PALYNOLOGY
2018, VOL. 42, NO. S1, 111–134
https://doi.org/10.1080/01916122.2018.1465736



# Taxonomic revision of *Spiniferites elongatus* (the resting stage of *Gonyaulax elongata*) based on morphological and molecular analyses

Nicolas Van Nieuwenhove[g,a], Éric Potvin[b], Maija Heikkilä[g,c], Vera Pospelova[d], Kenneth Neil Mertens[e], Edwige Masure[f], Małgorzata Kucharska[h], Eun Jin Yang[b], Nicolas Chomérat[e] and Marek Zajaczkowski[h]

[a]Department of Glaciology and Climate, Geological Survey of Denmark and Greenland, Copenhagen K, Denmark; [b]Department of Geoscience, Aarhus University, Aarhus, Denmark; [c]Division of Polar Ocean Environment, Korea Polar Research Institute, Incheon, Korea; [d]Environmental Change Research Unit (ECRU), Department of Environmental Sciences, University of Helsinki, Helsinki, Finland; [e]School of Earth and Ocean Sciences, University of Victoria, Victoria, BC, Canada; [f]Ifremer, LER BO, Station de Biologie Marine, Place de la Croix, Concarneau Cedex, France; [g]Université Pierre et Marie Curie-Paris, UMR-CNRS, Paris, France; [h]Department of Marine Ecology, Institute of Oceanology, Polish Academy of Sciences, Sopot, Poland

**ABSTRACT**

We restudied the morphological complex comprising the cyst-based species *Spiniferites elongatus*/*Spiniferites frigidus*/*Rottnestia amphicavata*. We reviewed existing studies, and acquired new morphometric measurements of recent cysts from across the Northern Hemisphere, scanning electron microscopy (SEM) observations of cysts from Barents Sea surface sediments, and genetic analyses of cysts from the Beaufort Sea. The measurements suggest that populations and morphospecies cannot be distinguished based on morphometric criteria. Furthermore, sequential sediment trap samples from Hudson Bay reveal that morphological variation can occur at the same location over a few weeks, arguing against a uniform morphological response to environmental parameters. The SEM observations reveal a consistent gonyaulacacean tabulation (Po, 4′, 6″, 6c, 5 s, *6‴, 1p, 1⁗). The small and large subunit ribosomal RNA genes and the internal transcribed spacer sequences obtained from differing cysts from the Beaufort Sea with morphologies attributable to the complex, including forms that correspond to *Rottnestia amphicavata*, were all identical and conform to those of *Gonyaulax elongata* from the Orkney Islands. The molecular analyses thus support the conclusion that the morphological variability is not reflected genetically and occurs within one species. Based on arguments against the generic attribution of *amphicavata* to *Rottnestia*, the continuum between the extreme ends of the morphological range, and the molecular data, we suggest *Rottnestia amphicavata* to be conspecific with *Spiniferites frigidus*, and both to be junior synonyms of *Spiniferites elongatus*. The morphometric data further indicate that *Spiniferites ellipsoideus*, an elongate cyst from the Miocene, can also be considered a junior synonym of *Spiniferites elongatus*. It is recommended to use two informal types in census work (i.e. *Spiniferites elongatus* – Beaufort morphotype for morphologies formerly assignable to *Spiniferites frigidus*/*Rottnestia amphicavata*, and *Spiniferites elongatus* – Norwegian morphotype for cysts with strongly reduced processes) to separate specimens at both extreme ends of the morphological spectrum from typical specimens of *Spiniferites elongatus*.

**KEYWORDS**

Single-cell PCR; *Spiniferites ellipsoideus*; *Spiniferites frigidus*; *Rottnestia amphicavata*; morphologic variability; taxonomy

## 1. Introduction

Elongate *Spiniferites* Mantell 1850 cysts constitute an important part of the modern dinoflagellate cyst (dinocyst) assemblages in sediments from the polar to temperate regions. Until now, four cyst species with an elongated central body have been defined from recent sediments: *Spiniferites lazus* Reid 1974 and *Spiniferites elongatus* Reid 1974 from intertidal sediment samples from the British Isles, *Spiniferites frigidus* Harland and Reid in Harland et al. 1980, and *Rottnestia amphicavata* Dobell and Norris in Harland et al. 1980, both from the Beaufort Sea in the Canadian Arctic. *Spiniferites lazus* can easily be distinguished from the latter three morphological types based on its characteristic fenestrate process bases, and is discussed elsewhere in this volume (Gurdebeke et al. 2018). In addition, the elongate species *Spiniferites ellipsoideus* Matsuoka 1983 was defined from mid to upper Miocene sediments from Japan based on its shorter and wider cyst body with respect to *Spiniferites elongatus* (as recognised at that time). Matsuoka (1983) argued that *Spiniferites ellipsoideus*, whose stratigraphic range goes down to the Middle Miocene (Matsuoka et al. 1987; Kurita and Ishikawa 2009) or possibly the Early Miocene (Matsuoka and Bujak 1988) and has not been recorded from sediments younger than the Early Pliocene (Matsuoka et al. 1987; Williams et al. 1993), might be an ancestral form of *Spiniferites elongatus*, which appeared during the Late Miocene together with *Spiniferites frigidus* (Matsuoka et al.

**CONTACT** Nicolas Van Nieuwenhove nicolas.vannieuwenhove@unb.ca Department of Earth Sciences, University of New Brunswick, Fredericton NB E3B 5A3, Canada.



Published online 14 Dec 2018

1987). In contrast to these long-ranging species, *Rottnestia amphicavata* has only been identified in Holocene sediments (Fensome et al. 2008).

The numerous observations of *Spiniferites elongatus* since its original description (see de Vernal et al. 2018, for details on the distribution) have revealed that the species can display a large morphological variability, to such a degree that it is hard to draw a clear line between *Spiniferites elongatus* and *Spiniferites frigidus*/*Rottnestia amphicavata* (see section 2.2 below). Consequently, it is a fairly common practice, especially in hemispheric and global datasets (de Vernal et al. 2001, 2005, 2013; Marret and Zonneveld 2003; Zonneveld et al. 2013), to group these three morphospecies as '*Spiniferites elongatus* sensu lato' – a term that will also be used here when referring to the general cyst morphology of the three species. Consequently, the question arises whether these morphological forms indeed constitute three distinct species or rather reflect the highly variable cyst morphology of one motile species. A first clue was provided by culture studies with *Spiniferites elongatus* cysts of variable morphology from three different locations in the North Atlantic Ocean, namely off Nova Scotia, the Orkney Islands, and the English North Sea coast (Ellegaard et al. 2003). Their culture studies revealed not only that the *Spiniferites elongatus* cysts all enclosed the same, until then undescribed, motile stage *Gonyaulax elongata* Ellegaard et al. 2003, but also that established cultures can subsequently form cysts whose morphology is quite different from the one they originally germinated from. In addition, Ellegaard et al. (2003) partially determined the gene sequence coding for the large subunit ribosomal RNA of a strain established after the excystment of a cyst collected from surface sediment of the Orkney Islands. The motile cells that germinated from the cysts collected from offshore Nova Scotia produced *Spiniferites frigidus*-like cysts, but as this strain was short lived and did not produce many cysts or motile cells, they could not verify whether these constitute a separate species or conform to *Spiniferites elongatus*/*Gonyaulax elongata* from the Orkney Islands.

Here, we review the known morphological variability and suspected links with environmental parameters of *Spiniferites elongatus*, *Spiniferites frigidus* and *Rottnestia amphicavata*, followed by the results of newly obtained morphometric data from 66 recent elongate cysts from across the Northern Hemisphere and scanning electron microscopy (SEM) observations of 24 cysts recovered from Barents Sea surface sediments that cover the morphological spectrum displayed by this species complex. The visual examination of the morphological variability is complemented by genetic analysis on nine elongate cysts of varying morphologies isolated from surface sediments from the Beaufort Sea. The single-cell polymerase chain reaction (PCR) technique has been commonly used to explore phylogenetic patterns in dinoflagellate cysts (e.g. Bolch 2001; Matsuoka et al. 2006; Kawami et al. 2009; Matsuoka et al. 2009; Mertens et al. 2012b, 2013; Gu et al. 2015), and has the potential to determine whether displayed variability is intra- or interspecific based on genetic distances (Litaker et al. 2007). Thus, the molecular sequences of the nine cysts, based on genes coding for the small and large subunit ribosomal RNA (SSU and LSU rDNA) as well as the internal transcribed spacer (ITS rDNA), are used to determine the relevance of morphological traits at the species level, and to compare the genetic fingerprint of the Beaufort Sea cysts with that of *Gonyaulax elongata* from the Orkney Islands (Ellegaard et al. 2003). We furthermore provide the emended description of *Spiniferites elongatus*. Also note that since only cyst and not theca morphological characteristics are discussed in this paper, the use of the prefix 'para-' is omitted.

## 2. Background

### 2.1. Original observations and descriptions

*Spiniferites elongatus* was formally described by Reid (1974) from recent coastal British sediments, after earlier, unspecified observations across the North Atlantic Ocean (e.g. Wall and Dale 1968; Harland and Downie 1969; see section 5). Along with the typical elongate shape, the species is described as having two high, hollow, trumpet-shaped complex processes at the ventral side of the antapical plate, high sutural flanges at the apex, and septa of variable height between the processes. Furthermore, Reid (1974) remarks the posteriorly widening sulcus without observable sulcal plates and a short complex process at the anterior side of the sulcus, as well as short gonal processes around the cingulum.

A few years after the formal description of *Spiniferites elongatus*, the similarly elongate cyst species *Spiniferites frigidus* and *Rottnestia amphicavata* were described from (sub-)recent sediments from the Canadian Arctic Ocean by Harland and Reid and by Dobell and Norris, respectively, in Harland et al. (1980). These two new species were distinguished from *Spiniferites elongatus* mainly by the development of the sutural membranes and septa: in *Spiniferites frigidus*, these are still variable in height, but conspicuous all over the cyst, sometimes completely including the processes, which are only discernible by their distal tips surmounting the crests in gonal positions. In *Rottnestia amphicavata*, the septa appear somewhat less developed but still conspicuous at the apex, and are particularly well developed at the antapex, where the 'antapical extension is elaborately folded delimiting two pericoels … separated from each other by an invagination of the periphragm … and connected to the exterior by a hydropyle' (i.e. a rounded opening) (Dobell and Norris in Harland et al. 1980, p. 219). Dobell and Norris considered the presence of a pair of pericoels, i.e. cavities between the endophragm and periphragm, to be a characteristic feature of *Rottnestia amphicavata*. However, they also described *Rottnestia amphicavata* var. B that had no invagination of the periphragm, thus having only one large antapical pericoel, and *Rottnestia amphicavata* var. C that had no well-developed sutural crests and processes (Harland et al. 1980). Dobbell and Norris (in Harland et al. 1980) further expressed that *Rottnestia amphicavata* differs from *Spiniferites frigidus* – and other *Spiniferites* species for that matter – in having three instead of four apical plates, in the details of the sulcal plates and in having a different shape of 6″ and 1‴. However, it needs to be pointed out that the 'flangy'

nature of *Rottnestia amphicavata* can hamper the observation of the paratabulation, as was also noted by Stover and Evitt (1978), who consequently suggested three or four apical plates in *Rottnestia* Cookson and Eisenack (1961).

### 2.2. Morphological variability across environmental domains

Already at the time of description, a continuous variation was noticed within and between the morphotype extremes of *Spiniferites elongatus* sensu lato (e.g. Harland et al. 1980, p. 222, p. 224). As specific morphologies appeared to be more common in particular environments, it was suggested that the morphological variability might be geographically and/or ecologically controlled (e.g. Harland 1982, 1983). This motivated Harland and Sharp (1986) to investigate, biometrically, the morphology of elongate cysts at three different settings in the northern North Atlantic Ocean: an estuarine locality in Scotland (i.e. Firth of Forth; sea surface salinity (SSS) = 34, winter sea surface temperature (wSST) = 3–5 °C, summer sea surface temperature (sSST) = 13–14 °C), the Norwegian Sea (SSS = 35–36, wSST = 0–10 °C, sSST = 10–20 °C), and the Barents Sea (SSS = 32–34, wSST = 0–5 °C, sSST = 0–10 °C). Their observations appeared to confirm the original notions: specimens from the coastal British setting corresponded closely to the original description of *Spiniferites elongatus* from a similar setting, with morphological variability limited to the height and size of the sutural membranes. The cold-spectrum specimens from the Barents Sea had more strongly developed sutural membranes that often incorporate the processes, their distal tips sitting on top of the membranes. While Harland and Sharp (1986) refer to these specimens as *Spiniferites elongatus*, they had indeed been identified originally as *Spiniferites frigidus* by Harland (1982). In addition, the specimens from the Norwegian Sea included a morphotype at the other end of the 'flamboyancy spectrum'. These specimens, referred to as *Spiniferites* cf. *elongatus* by Harland and Sharp (1986), display reduced membranes and more conical, short to stout processes (see their pl. I, figs 11–14). Similar and even more strongly reduced *Spiniferites* cf. *elongatus* morphotypes have since only been observed and explicitly reported as such from last interglacial sediments from the Norwegian Sea (Van Nieuwenhove et al. 2008) (Plate 6).

Harland and Sharp (1986) supported their qualitative observations with semi-quantitative analysis of cyst morphology, through measuring cyst width and length as well as membrane and process height. [Note that the values shown by Harland and Sharp (1986, their table 1) for 'antapical membrane length' are often nearly twice the highest values measured here for that parameter. As such, it seems that they measured the longest part of the antapical membrane, and not the central height in the middle of the membrane as done here.] While based on a fairly low number of measurements and consequently statistically inconclusive, cysts from the Norwegian Sea seem to be generally smaller and less membranous than those from the Barents Sea, with the typical *Spiniferites elongatus* cysts from the Scottish estuarine setting falling between the two ranges. Although cautious about making unsubstantiated conclusions, Harland and Sharp (1986) felt that it was possible, at least subjectively, to separate populations from the three geographic locations and, thus, differing environmental conditions.

No morphometric studies on elongate *Spiniferites* have been attempted since the work by Harland and Sharp (1986). The considerable overlap in their plots suggests that morphometrics is an unlikely criterion for differentiating the three morphospecies, but also that, nonetheless, simple measurements might be useful in past environmental reconstructions, for instance through sample population scatter plots or frequency spectra (cf. Ellegaard 2000). Indeed, it should be noted that a single morphology virtually never makes up the entire *Spiniferites elongatus* sensu lato population in a given area; rather, the proportions of the different morphologies that make up the total *Spiniferites elongatus* sensu lato population seem to change from one region to another. An increase in available measured morphological data may reveal whether or not there is a quantifiable relationship between the morphology of elongate *Spiniferites* cysts and sea surface parameters, similar to what has been shown for the cysts of *Protoceratium reticulatum* (Claparède and Lachmann 1859) Bütschli 1885 (*Operculodinium centrocarpum* sensu Wall and Dale 1966) and *Lingulodinium polyedra* (Stein 1883) Dodge 1989 (*Lingulodinium machaerophorum* (Deflandre and Cookson 1955) Wall 1967) (e.g. Mertens et al. 2009, 2011, 2012a; Jansson et al. 2014; Sildever et al. 2015). Alternatively to environmental steering, the relative increase of specific morphologies could also be a result of isolation and differentiation of distant populations.

## 3. Material and methods

### 3.1. Morphometric analysis

In order to expand the morphometric analysis initiated by Harland and Sharp (1986) to areas outside the northern North Atlantic, measurements were made on a total of 66 *Spiniferites elongatus* sensu lato cysts recovered from surface sediments from Hudson Bay (n = 14); New England, USA (n = 3); off Newfoundland, Canada (n = 6); Omura Bay, Nagasaki Prefecture, Japan (n = 2); the Alaskan coast (n = 1); the Santa Barbara Basin, California, USA (n = 1); the northern Bering Sea (n = 7); and the Chukchi Sea (n = 12); as well as sediment traps deployed in eastern (n = 10) and western (n = 5) Hudson Bay in November–December 2005, and eastern Hudson Bay in July 2006 (n = 5). When orientation permitted, measurements were made of cyst width and length, antapical process length, and height of the antapical crest, as illustrated in Plate 2, figure 1. The measurements are shown in Table 1. Apart from the Santa Barbara Basin (Pospelova et al. 2006), New England (Pospelova et al. 2004), and Hudson Bay assemblages (Heikkilä et al. 2014, 2016), the measured cysts belong to unpublished records. The palynological preparation protocol from the aforementioned publications was followed.

**Table 1.** Results from the morphometric analyses of *Spiniferites elongatus* sensu lato cysts retrieved from surface sediments and sediment trap sequences.

| | Area | Production window | Cyst height (μm) | Cyst width (μm) | Antapical process length (μm) | Antapical crest height (μm) |
|---|---|---|---|---|---|---|
| 1 | Western Hudson Bay | November–December 2005 | 47 | 27 | 9 | N/A |
| 2 | | | 47 | 31 | 12 | 4 |
| 3 | | | 56 | 29 | 13 | N/A |
| 4 | | | 49 | 29 | 8 | N/A |
| 5 | | | 48 | 31 | 9 | N/A |
| 6 | Eastern Hudson Bay | November–December 2005 | 57 | 29 | 15 | N/A |
| 7 | | | 52 | 26 | 5 | 3 |
| 8 | | | 46 | 31 | 8 | 2 |
| 9 | | | 55 | 31 | 7 | 4 |
| 10 | | | 54 | 32 | 14 | 3 |
| 11 | | | 60 | 35 | 8 | N/A |
| 12 | | | 52 | 31 | 18 | 3 |
| 13 | | | 54 | 28 | 15 | 4 |
| 14 | | | 53 | 33 | 16 | 3 |
| 15 | | | 47 | 33 | 5 | N/A |
| 16 | | July 2006 | 54 | 33 | 9 | 5 |
| 17 | | | 49 | 33 | 14 | 4 |
| 18 | | | 58 | 32 | 15 | 7 |
| 19 | | | 50 | 34 | 14 | 9 |
| 20 | | | 50 | 28 | 22 | 4 |
| 21 | Hudson Bay | Surface sediment | 61 | 36 | 10 | N/A |
| 22 | | | 49 | 36 | 15 | 3 |
| 23 | | | 49 | 31 | N/A | N/A |
| 24 | | | 52 | 34 | 10 | 4 |
| 25 | | | 51 | 38 | 14 | 7 |
| 26 | | | 51 | 26 | 11 | 8 |
| 27 | | | 58 | 35 | 12 | 5 |
| 28 | | | 61 | 35 | 20 | 6 |
| 29 | | | 62 | 35 | 16 | 6 |
| 30 | | | 56 | 34 | 17 | 3 |
| 31 | | | 52 | 32 | 12 | 7 |
| 32 | | | 54 | 38 | 16 | 11 |
| 33 | | | 51 | 32 | 9 | 6 |
| 34 | | | 48 | 33 | 17 | 9 |
| 35 | New England | Surface sediment | 59 | 36 | 13 | 8 |
| 36 | | | 49 | 25 | 15 | 3 |
| 37 | | | 47 | 33 | 9 | 5 |
| 38 | Newfoundland | Surface sediment | 53 | 31 | 10 | 6 |
| 39 | | | 54 | 36 | 12 | 4 |
| 40 | | | 42 | 27 | 12 | 3 |
| 41 | | | 53 | 32 | 15 | 2 |
| 42 | | | 57 | 32 | 13 | 6 |
| 43 | | | 55 | 35 | 14 | 4 |
| 44 | Omura Bay | Surface sediment | 47 | 23 | 9 | N/A |
| 45 | | | 56 | 30 | 12 | 3 |
| 46 | Alaskan coast | Surface sediment | 42 | 26 | 10 | 6 |
| 47 | Santa Barbara Basin | Surface sediment | 46 | 26 | 11 | 2 |
| 48 | North Bering Sea | Surface sediment | 48 | 32 | 12 | 6 |
| 49 | | | 48 | 27 | 12 | 4 |
| 50 | | | 56 | 25 | 14 | 8 |
| 51 | | | 46 | 27 | 10 | 8 |
| 52 | | | 52 | 34 | 11 | 7 |
| 53 | | | 51 | 33 | 17 | 12 |
| 54 | | | 50 | 33 | 12 | 8 |
| 55 | Chukchi Sea | Surface sediment | 53 | 35 | 18 | 10 |
| 56 | | | 53 | 38 | 10 | 6 |
| 57 | | | 64 | 31 | 15 | 10 |
| 58 | | | 51 | 41 | 18 | 8 |
| 59 | | | 60 | 37 | 10 | N/A |
| 60 | | | 58 | 37 | 15 | 8 |
| 61 | | | 61 | 36 | 21 | 3 |
| 62 | | | 63 | 35 | 20 | 6 |
| 63 | | | 49 | 30 | 14 | 8 |
| 64 | | | 50 | 32 | 17 | 6 |
| 65 | | | 60 | 39 | 17 | 5 |
| 66 | | | 52 | 31 | 16 | 6 |


**Plate 1.** Bright-field photomicrographs of the *Spiniferites elongatus* sensu lato cysts isolated from the Beaufort Sea that were used in the genetic analyses. The National Center for Biotechnology Information (NCBI) GenBank accession numbers associated to the specimens are KU358942 (cyst 1), KU358943 (cyst 2), KU358944 (cyst 3), KU358945 (cyst 4), KU358946 (cyst 5), KU358947 (cyst 6), KU358948 (cyst 7), KU358949 (cyst 8), and KU358950 (cyst 9). Scale bars = 10 μm.

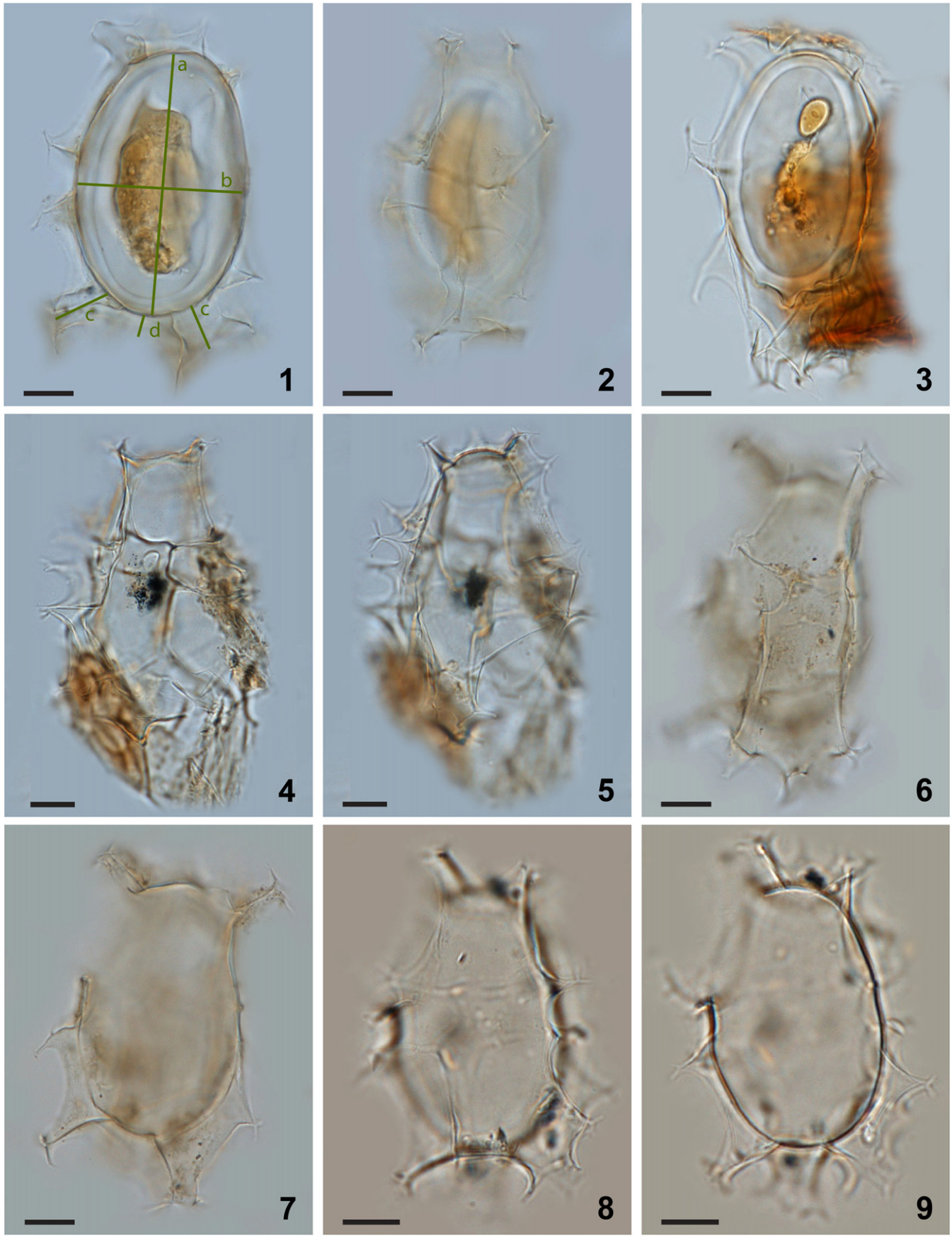


**Plate 2.** Bright-field photomicrographs of *Spiniferites elongatus* from off Newfoundland (1–2, 3, 4–5, 6–7) and the Alaskan Coast (8–9). The lines in figure 1 indicate how cyst morphometrics were measured. a = cyst length, b = cyst width, c = antapical process length, d = antapical membrane height. Scale bars = 10 μm.

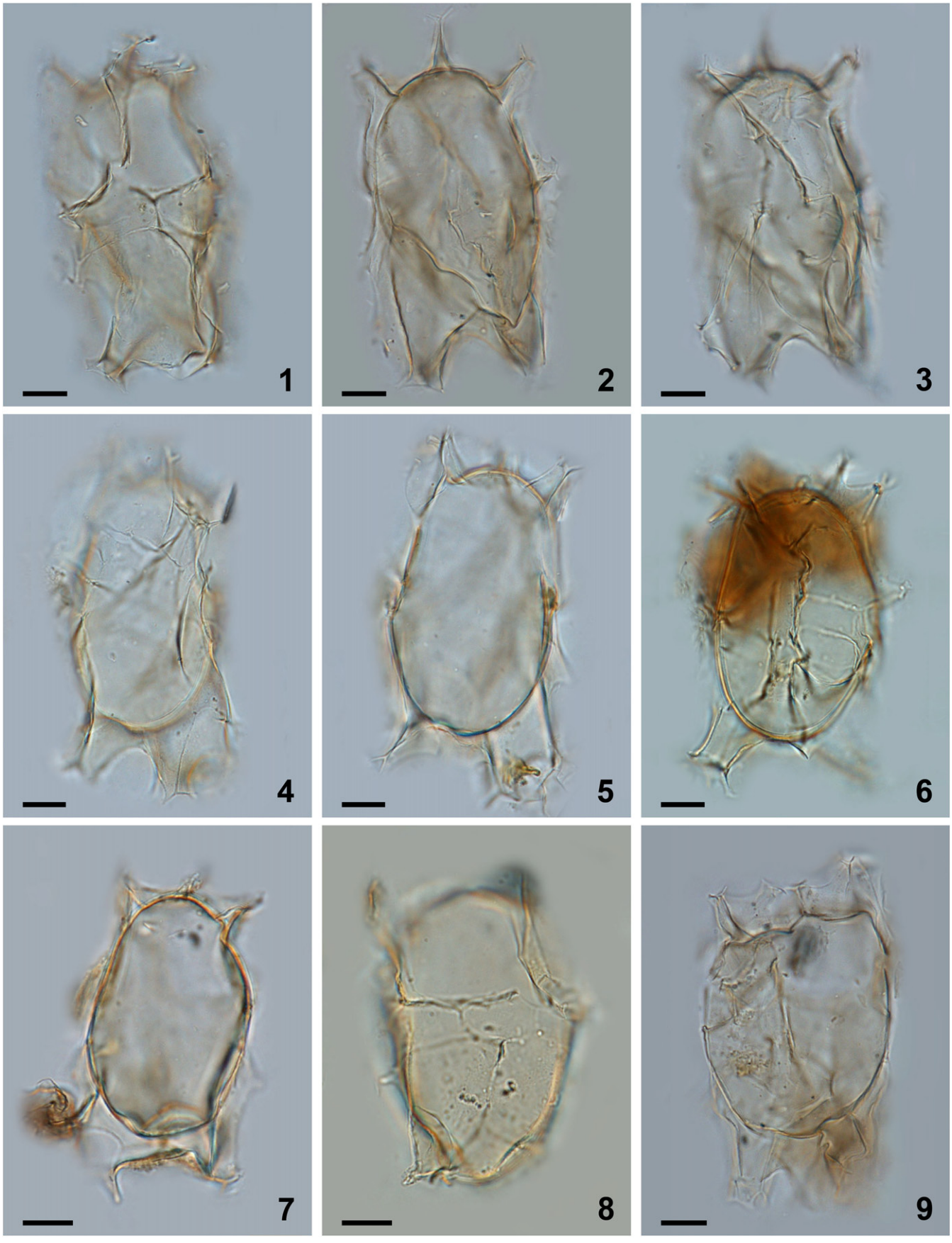


**Plate 3.** Bright-field photomicrographs of *Spiniferites elongatus* from Chukchi Sea. 1–3. Dorsal, optical section, and ventral view of a specimen with a high membrane between the two dorsal antapical processes. 4–5. Specimen illustrating the unequal development of the dorsal antapical processes. 6–9. Further illustration of the morphological variability of specimens in a single assemblage. Scale bars = 10 μm.

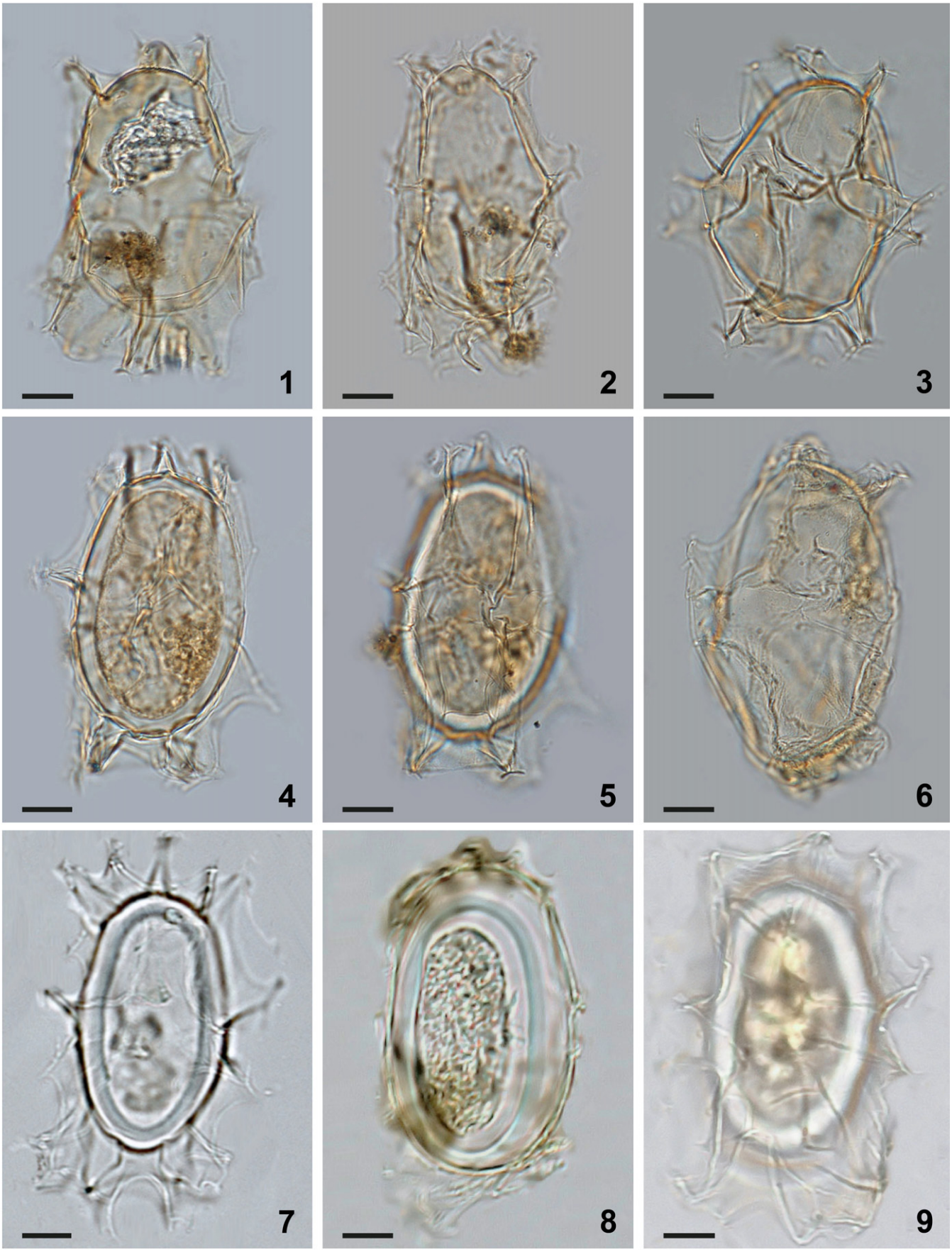


**Plate 4.** Bright-field photomicrographs of *Spiniferites elongatus* from (1–6) Hudson Bay surface sediments, (7) eastern Hudson Bay sediment trap deposits collected over July 2006, and (8, 9) western Hudson Bay sediment trap deposits collected from November to December 2005. Note the marked antapical suturocavation in the specimen in figure 7, and the differences in morphology between cysts produced over the same growing season (8 and 9). Figures 1 and 9 are examples of specimens that can be identified as *Spiniferites elongatus* – Beaufort morphotype. Scale bars = 10 μm.

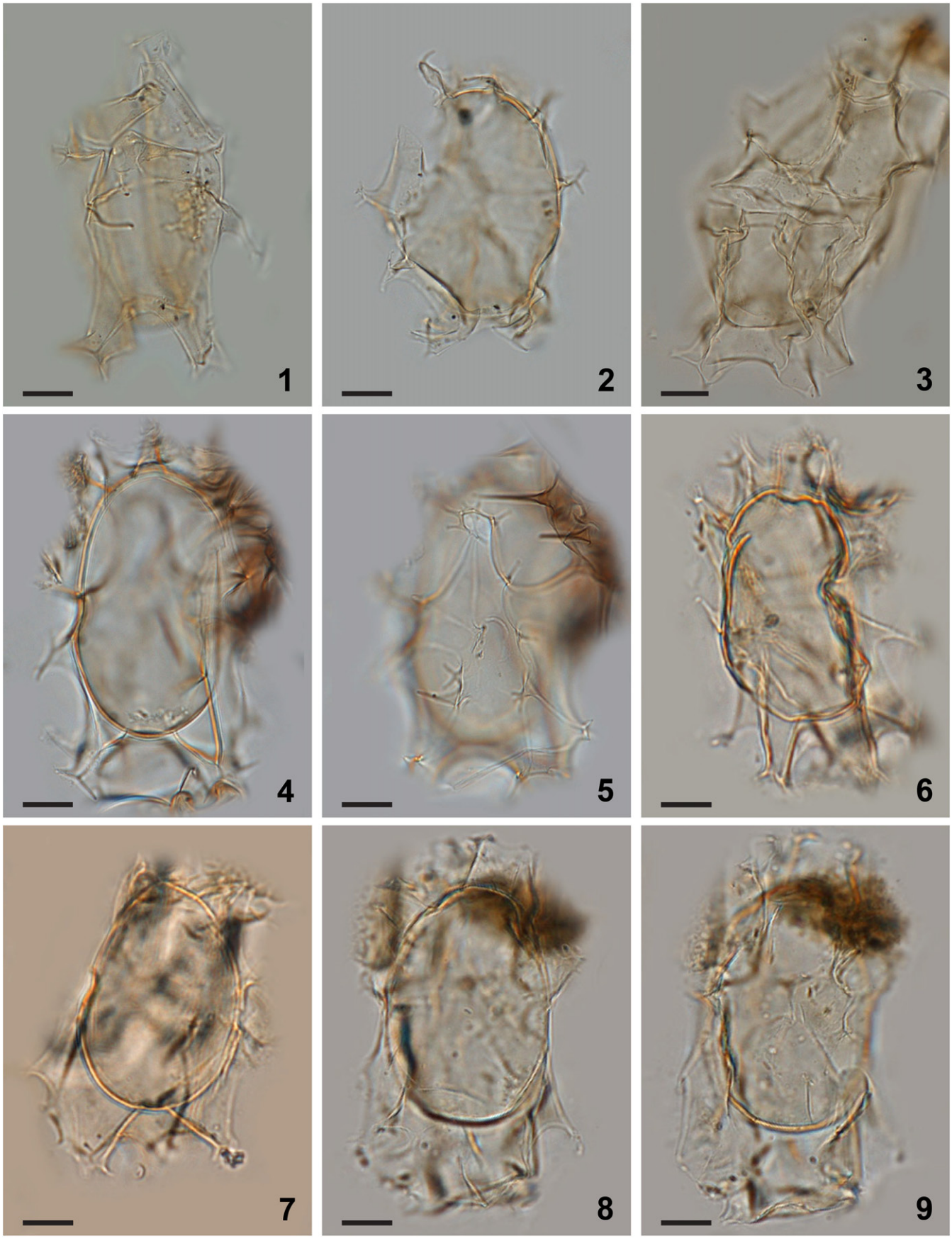


**Plate 5.** Bright-field photomicrographs of *Spiniferites elongatus* sensu lato from New England (1, 2, 3), Omura Bay, Japan (4, 5), and the Bering Sea (6–9). While the specimens shown in figures 7–9 are good examples of *Spiniferites elongatus* – Beaufort morphotype, the specimens shown in figures 4–6 illustrate morphologies somewhat intermediate between typical *Spiniferites elongatus* and the Beaufort morphotype. Scale bars = 10 μm.

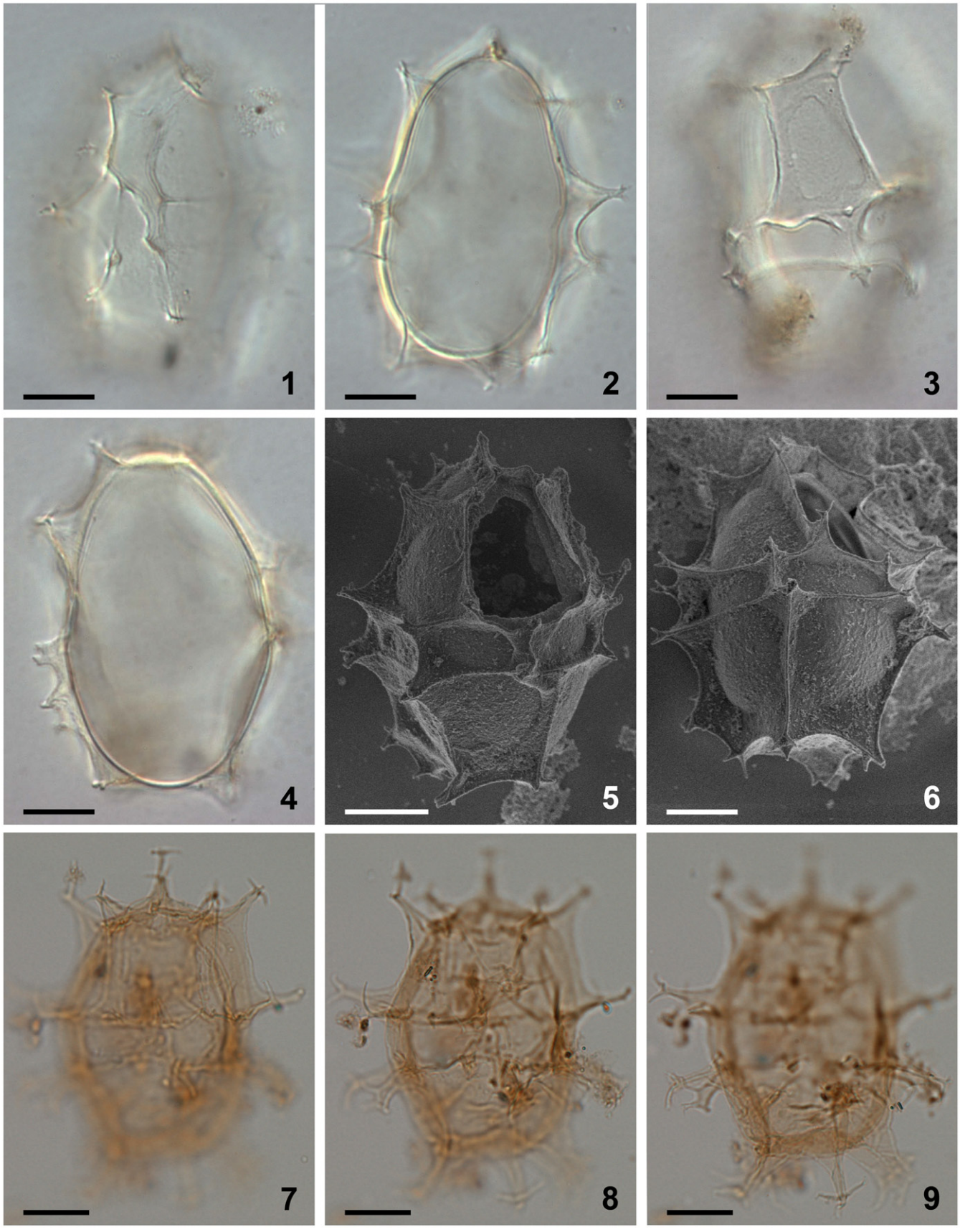


**Plate 6.** 1–6. Dual interference photomicrographs (1–4) and scanning electron micrographs (5, 6) of *Spiniferites elongatus* – Norwegian morphotype, from late Pleistocene (Marine Isotope Stage 5e) sediments from the Vøring Plateau, Norwegian Sea. 7–9. Newly produced photomicrographs of the Miocene specimen from Japan that had been designated the holotype of *Spiniferites ellipsoideus*, herein considered a junior synonym of *Spiniferites elongatus*. Figures 7–9 courtesy of Kazumi Matsuoka, with kind permission. Scale bars = 10 μm.

### 3.2. Cyst observation and micrographic documentation

The micrographs of the nine cysts selected for molecular analysis (Plate 1) were taken with an AxioCam HRc digital camera mounted on an Axio Imager A2 microscope (Carl Zeiss Microscopy GmbH, Göttingen, Germany) at the Korea Polar Research Institute. The micrographs in the other plates were obtained with a Nikon Eclipse 80i microscope and coupled Nikon DS camera head (DS-Fi1)/DS camera control unit DS-L2 (Nikon, Japan) at the Paleoenvironmental/Marine Palynology Laboratory, University of Victoria, Canada (Plates 2, 3, 4, figures 1–6, 5); an AxioCamMRc5 camera mounted on a Zeiss Axio10 transmitting light microscope at the Microscopy Facility of the Department of Geosciences and Geography, University of Helsinki (Finland) (Plate 4, figures 7–9); and an AxioCam digital camera mounted on a Zeiss Axiophot transmitting light microscope at the GEOMAR Helmholtz Centre for Ocean Research Kiel, Germany (Plate 6). The scanning electron micrographs in Plate 6 were obtained using a Hitachi S-3400N type II scanning electron microscope at Geotop, Montreal, Canada.

For detailed analyses of cyst tabulation and morphology by means of SEM, 24 cysts of varying morphology were isolated from a 10-cm-long core collected in the Barents Sea (75°55.078′ N, 30°14.454′ E; 310 m water depth) in August 2015 during a cruise of RV *Oceania* (Institute of Oceanology, Polish Academy of Sciences). The core was cut into 1-cm-thick slices and stored in a refrigerator before standard palynological preparation, as follows: After determining the wet and dry weight, ~4 $cm^3$ of sediment was treated with cold 10% hydrochloric acid (HCl) for 24 hours. The residue was then wet sieved to recover the fraction between 15 µm and 125 µm, which was subsequently treated with cold 40% hydrofluoric acid (HF) for 48 hours, and, after a short round of ultrasonication, sieved again through a sieve with a mesh

**Table 2.** Location and local surface water conditions for the Beaufort Sea surface sediment samples from which cysts of *Spiniferites elongatus* sensu lato were isolated.

| Station number | Latitude (N) | Longitude (W) | Depth (m) | Temperature[a] (°C) | Salinity[a] | Cyst[b] |
|---|---|---|---|---|---|---|
| ARA05C07 | 70°27.540 | 135°46,962 | 56 | 6.69 | 29.40 | 1, 2, 5, 6, 7, 9 |
| ARA05C05 | 70°23.766 | 135°18,816 | 60 | 7.22 | 28.82 | 3, 4, 8 |

[a]Surface water condition.
[b]Numbers correspond to the specimens characterised genetically and illustrated in Plate 1.

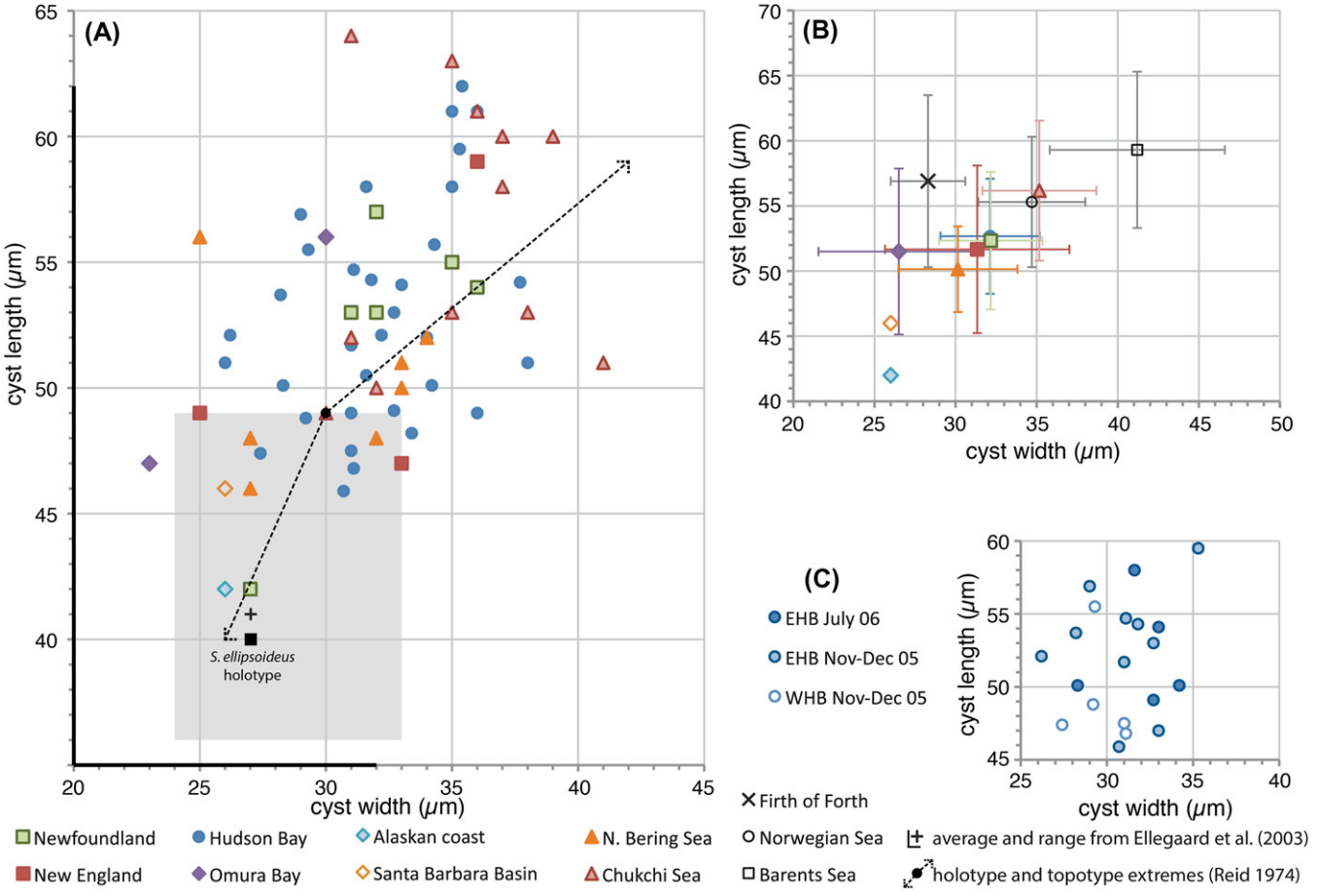


**Figure 1.** Scatter diagram showing cyst width against cyst length for measured elongate *Spiniferites* cysts. A, Data for all individual measurements from surface sediments. Also shown are the cyst width and length of the holotype of *Spiniferites elongatus* (black dot) and the topotype extremes (dashed arrow) (Reid 1974), and the average (black Greek cross) and range (black thickened axes) of the cysts measured by Ellegaard et al. (2003), as well as the cyst width and length of the holotype of *Spiniferites ellipsoideus* (black square) and its type assemblage (grey shaded area) (Matsuoka 1983). B, Average values for each regional surface sediment assemblage, with the standard deviation indicated. Also shown are the values from Harland and Sharp (1986) for specimens recovered from the Firth of Forth (UK), and the Norwegian and Barents seas. C, Individual measurements for the specimens recovered from sediment traps in eastern (EHB) and western (WHB) Hudson Bay.

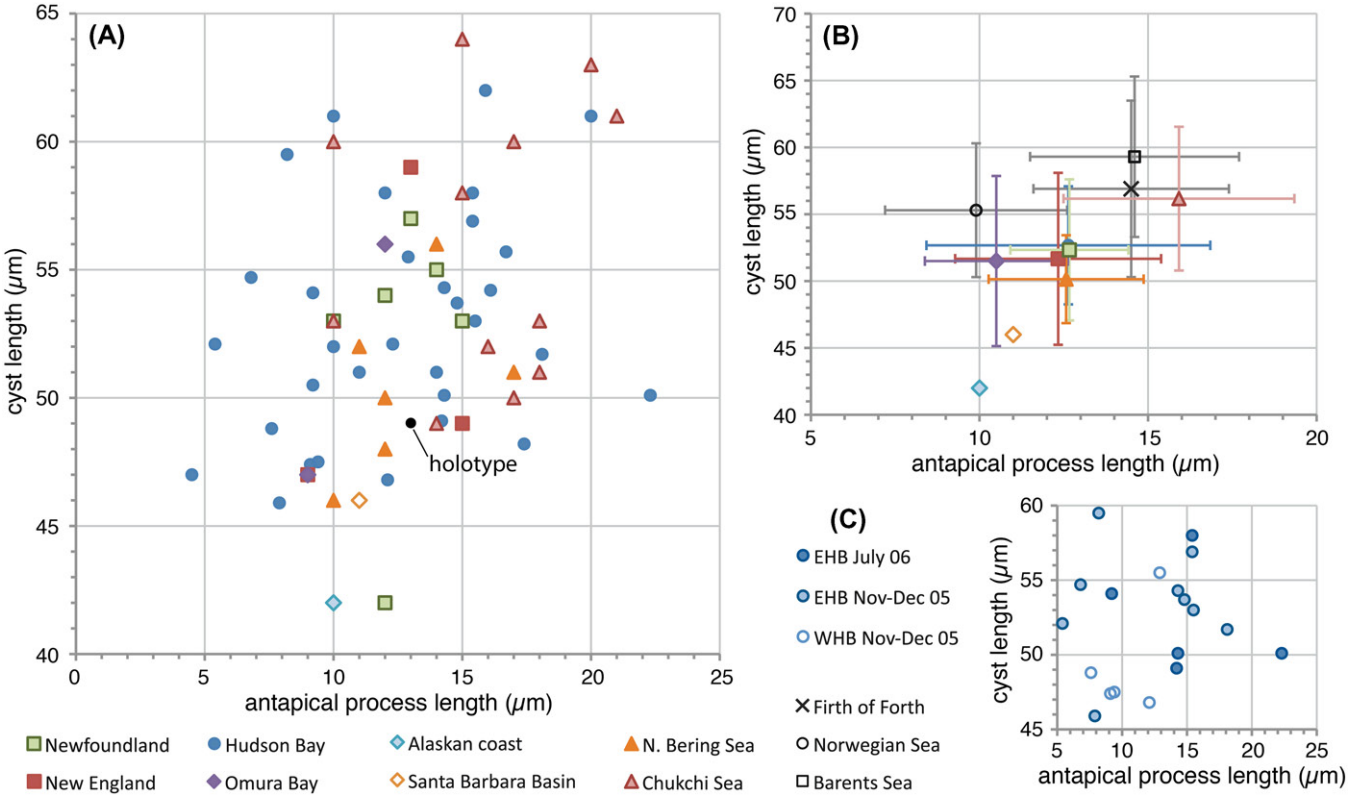


**Figure 2.** Scatter diagram showing antapical process length against cyst length for measured elongate *Spiniferites* cysts. A, Data for all individual measurements from surface sediments. The holotype is shown for reference (black dot). B, Average values for each regional surface sediment assemblage, with the standard deviation indicated. Also shown are the values from Harland and Sharp (1986) for specimens recovered from the Firth of Forth (UK), and the Norwegian and Barents seas. Note that the 'antapical membrane length' given by these authors (Harland and Sharp 1986, their table 1) is considered to correspond the antapical process length as measured here. C, Individual measurements for the specimens recovered from sediment traps in eastern (EHB) and western (WHB) Hudson Bay.

diameter of 15 μm. No oxidation was performed. Single specimens were picked from the residue under an inverted microscope with a micropipette into 0.2-mL tubes containing distilled water. The tubes were filtered using polycarbonate membrane filters (Millipore GTTP Isopore, 0.22 μm pore size, Millipore, Billerica, MA, USA), rinsed in deionised water and air dried. After gold-coating, the examination was performed using a FEI Quanta 200 scanning electron microscope with an electron acceleration of 2.5 to 5 kV at IFREMER (Brest, France). The Kofoid System is used for plate labeling.

### 3.3. Cyst isolation for molecular analyses

Living dinoflagellate cysts were isolated for molecular analyses from surface sediment samples collected on 1 September 2014 from the Beaufort Sea (Table 2) onboard the IBRV *Araon* during the ARA05C cruise. The surface sediment was retrieved with a boxcore and stored in the dark at 4 °C until further analyses. To concentrate living dinoflagellate cysts, 1 to 2 $cm^3$ of sediment was sonicated for 5 min in filtered seawater and sieved through 100 μm and 20 μm Nytex meshes. The 20–100 μm fraction was then transferred to a 100-mL beaker with filtered seawater. A manual vortex was applied and the suspended fraction was recovered. This fraction was then sonicated once more for 5 min and rinsed on the 20-μm Nytex mesh with filtered seawater to further rinse the cyst fraction.

The residue was observed with an Olympus IX73 inverted transmitted light microscope (Tokyo, Japan). Nine live cysts attributable to *Spiniferites elongatus* sensu lato were recovered from the sediment; their size and process length, and the extension of the sutural crests, vary from almost no ornamentation (Plate 1, figure 1) to morphotypes whose morphology corresponds to the description of *Spiniferites elongatus/Rottnestia amphicavata* (Plate 1, figures 7–9). The cells were transferred individually into a drop of filtered seawater framed by vinyl tape on a glass microscope slide, and sealed by applying silicon grease on the vinyl frame and covering the latter with a coverslip (modified from Horiguchi et al. 2000). Each cyst used in molecular analyses was photographed to record its morphological features (Plate 1).

### 3.4. Single-cyst rDNA sequencing and phylogenetic analyses

The living cysts were then washed in three drops of Milli-Q® Direct 8 water (EMD Millipore, Darmstadt, Germany) and broken with a glass micropipette. Drops containing cellular contents were then placed in microtubes and amplified directly.

Amplicons of the SSU rDNA, ITS rDNA, and LSU rDNA regions were obtained following nested PCR protocols. The first PCR round final mix concentrations were as follows: 1X PCR Ex Taq buffer (Takara Bio Inc., Seoul, Korea), 0.2 mM of dNTP (Takara Bio Inc., Seoul, Korea), 0.4 μM of each primer,

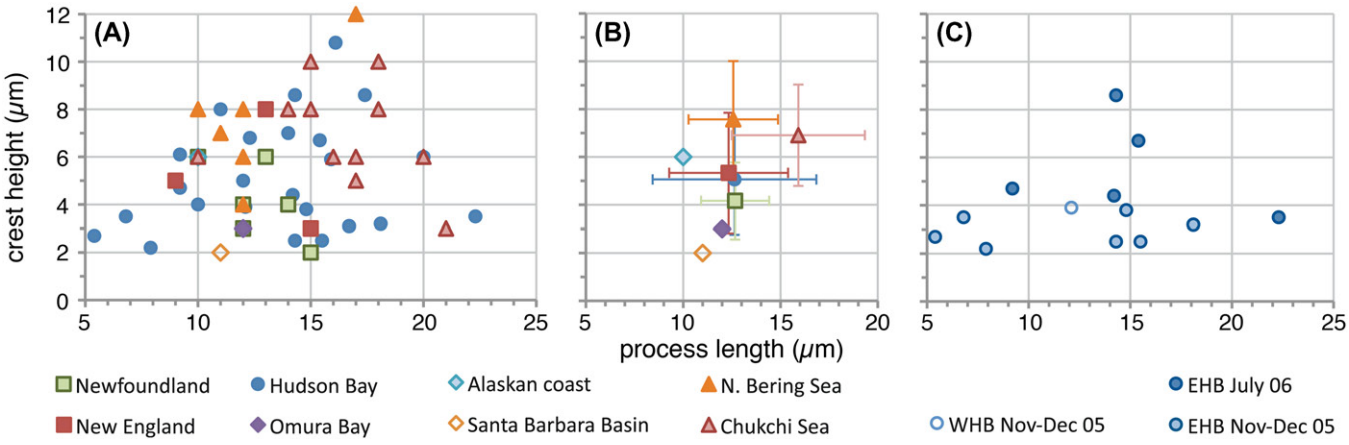


**Figure 3.** Scatter diagram showing antapical process length against antapical crest height for measured elongate *Spiniferites* cysts. A, Data for all individual measurements from surface sediments. B, Average values for each regional surface sediment assemblage, with the standard deviation indicated. C, Individual measurements for the specimens recovered from sediment traps in eastern (EHB) and western (WHB) Hudson Bay.

and 0.025 U $\mu L^{-1}$ of Ex Taq DNA polymerase (Takara Bio Inc., Seoul, Korea). EUKA and 28-1483 R primers (Medlin et al. 1988; Daugbjerg et al. 2000) were used in the first round of PCR to amplify the SSU rDNA, ITS rDNA, and LSU rDNA in a final volume of 50 μL. PCR was conducted using a thermal cycler (Takara Bio Inc., model TP350, Australia, Victoria) as follows: one activation step at 95 °C for 2 min, followed by 35 cycles at 95 °C for 20 s, 50 °C for 40 s, and 72 °C for 4 min 30 s, and a final elongation step at 72 °C for 10 min. A volume of 1 μL of the first PCR step was used as template for the second PCR round using the same mix. Individual reactions in a final volume of 50 μL were produced with these primer pairs and their corresponding annealing temperature (AT): EUKA and G23R (AT = 50 °C), G19F and G18R (AT = 51 °C), G17F and 5.8SR (AT = 51 °C), G22F and 5.8SR (AT = 53 °C), ITSF2 and ITSR2 (AT = 54 °C), 5.8SF and LSUB (AT = 51 °C), and LSU500F and 28-1483 R (AT = 53 °C) (Medlin et al. 1988; Daugbjerg et al. 2000; Litaker et al. 2003). The second round of PCR consisted of one activation step at 95 °C for 2 min, followed by 35 cycles at 95 °C for 20 s, AT for 40 s and 72 °C for 1 min, and a final elongation step at 72 °C for 5 min.

Positive and negative controls were used for all amplification reactions. The size of the amplicons was verified on a 1.0% agarose gel. Products were visualised under a UV lamp. The PCR products were purified using the Doctor Protein MGTM PCR SV DNA purification kit (MGmed, Inc., Seoul, Korea) according to the instructions of the manufacturer. The purified PCR products were sent to Macrogen Inc. (Seoul, Korea) where they were sequenced on an ABI PRISM® 3700 DNA Analyzer (Applied Biosystems, Foster City, CA, USA) with the primers used in the second round of PCR. The sequence fragments were assembled by manual alignment using BioEdit v. 7.0.9.0 (Hall 1999). The sequences obtained from the cysts were deposited in National Center for Biotechnology Information (NCBI) GenBank under the accession numbers KU358942 to KU358950.

The sequence of *Gonyaulax elongata* from Kirkwall Bay, Orkney Islands, Scotland, United Kingdom (Ellegaard et al. 2003), obtained from NCBI GenBank under the accession number AY154964 was used for comparison with our new sequences. Only four sequences out of nine of *Spiniferites elongatus* sensu lato from the Beaufort Sea were fully comparable to the partial LSU rDNA sequence from the Orkney Islands encompassing 1348 nucleotides.

The sequences of taxa used to construct the phylogenies were also obtained from NCBI GenBank. Our new and reference sequences were aligned using CLUSTAL X v. 2.0 (Larkin et al. 2007). The alignment was inspected and refined manually using BioEdit v. 7.0.9.0 (Hall 1999). The aligned matrix covers most of the LSU rDNA from domains 1 to 4 as defined by Lenaers et al. (1989) for *Prorocentrum micans* Ehrenberg 1834. However, a highly divergent region between domains 2 and 3 was partially removed because a reliable alignment was not always possible. Furthermore, based on the alignment, it was possible to include only five sequences obtained from the Beaufort Sea without reducing the length of the alignment. The TIM3 + G model of nucleotide substitution was selected by jModelTest v. 2.1.10 (Darriba et al. 2012) based on the corrected Akaike information criterion. The parameters for the model were as follows: assumed nucleotide frequencies A = 0.2879, C = 0.1762, G = 0.2657, and T = 0.2702; substitution rate matrix with G-T = 1.0000, A-C = 0.6214, A-G = 2.6837, A-T = 1.0000, C-G = 0.6214, C-T = 6.0515; proportion of invariable sites = 0.0000 and rates for variable sites assumed to follow a gamma distribution with shape parameter = 0.4450. The matrix was then analysed with PhyML v. 3.1 (Guindon et al. 2010) with the model previously selected to determine the maximum likelihood (ML) tree and to calculate the ML bootstrap values with 1000 replicates.

The matrix was also analysed with MrBayes v. 3.2.3 (Ronquist and Huelsenbeck 2003) for Bayesian analyses. The model previously selected by jModelTest v. 2.1.10 was used. Four independent Markov chain Monte Carlo simulations were run simultaneously for 2,000,000 generations. Trees were sampled every 1000 generations and the first 800 trees were deleted to ensure that the likelihood had reached convergence. A majority-rule consensus tree was created from

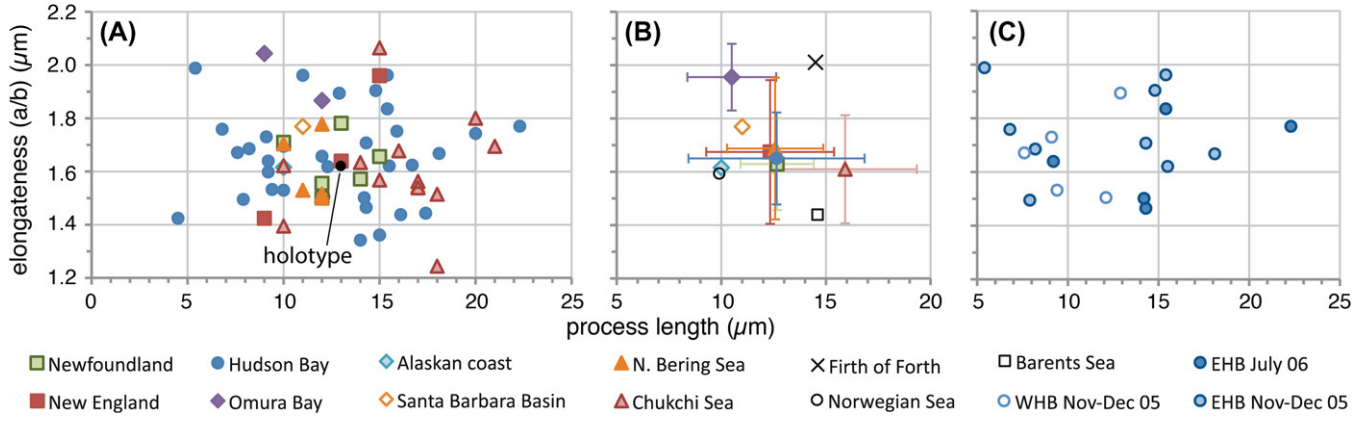


**Figure 4.** Scatter diagram showing antapical process length against elongateness (i.e. the ratio between cyst length and cyst width) for measured elongate *Spiniferites* cysts. The holotype is shown for reference (black dot). A, Data for all individual measurements from surface sediments. B, Average values for each regional surface sediment assemblage, with the standard deviation indicated. Also shown are the values from Harland and Sharp (1986) for specimens recovered from the Firth of Forth (UK), and the Norwegian and Barents seas. C, Individual measurements for the specimens recovered from sediment traps in eastern (EHB) and western (WHB) Hudson Bay.

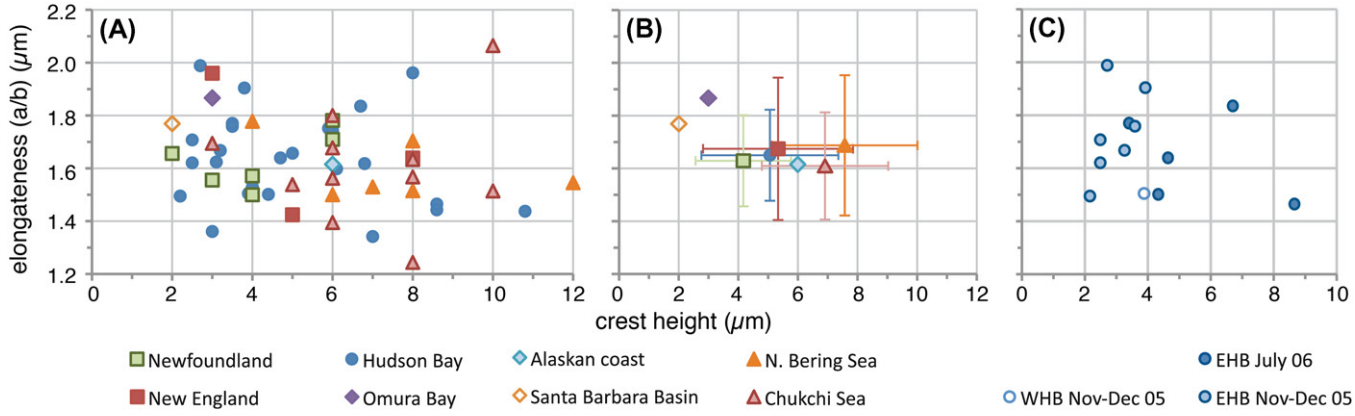


**Figure 5.** Scatter diagram showing antapical crest height against elongateness (i.e. the ratio between cyst length and cyst width) for measured elongate *Spiniferites* cysts. A, Data for all individual measurements from surface sediments. B, Average values for each regional surface sediment assemblage, with the standard deviation indicated. C, Individual measurements for the specimens recovered from sediment traps in eastern (EHB) and western (WHB) Hudson Bay.

the remaining 1201 trees to examine the posterior probabilities of each clade.

## 4. Results and discussion

### 4.1. Morphometry of the Spiniferites elongatus complex

The limited dataset of measurements presented here reveals important overlap between specimens from the different regions in all recorded morphometric parameters (Figures 1–5). Thus, geographical populations cannot be distinguished unambiguously based on morphometric parameters. The few 'Pacific' specimens from the Santa Barbara Basin and the Alaskan Coast that were measured (four) appear to be somewhat smaller and, particularly, narrower (Figure 1B), albeit this does not result in differences in general morphology (e.g. elongateness, Figure 4B) and more data are obviously needed to assess whether the size difference is statistically significant. Similarly, the smaller size of *Spiniferites ellipsoideus* (Plate 6, figures 7–9) as a distinguishing character (Matsuoka 1983) does not appear a valid criterion to separate *Spiniferites ellipsoideus* from *Spiniferites elongatus* sensu lato, as there is considerable overlap in the size spectrum of the type population of *Spiniferites ellipsoideus* and that of the modern *Spiniferites elongatus* sensu lato populations (Figure 1A).

Specimens from the Arctic shelf seas (Chukchi and Bering Sea) appear to be situated at the higher end of the 'flanginess' spectrum (crest height and process length), and the lower latitude specimens (Santa Barbara Basin, Omura Bay) are situated at the opposite end (Figure 3). This is also illustrated by the frequency distribution diagrams, which show that the Chukchi and Bering Sea populations appear to have (slightly) longer antapical processes and crests with respect to the total dataset (Figure 6C,D). Interestingly, specimens from the Barents Sea shelf also appear to be characterised by generally longer antapical processes (Figure 2B; Harland et al. 1980; note that those authors measured the antapical crest height differently, impeding comparison with our data). Hence, it would appear that there is a possible environmental control on the cyst morphology. However, the sediment trap data from Hudson Bay show that a wide range of morphologies are produced over a short period of relatively stable conditions (Figures 1–5; Plate 4), thus arguing

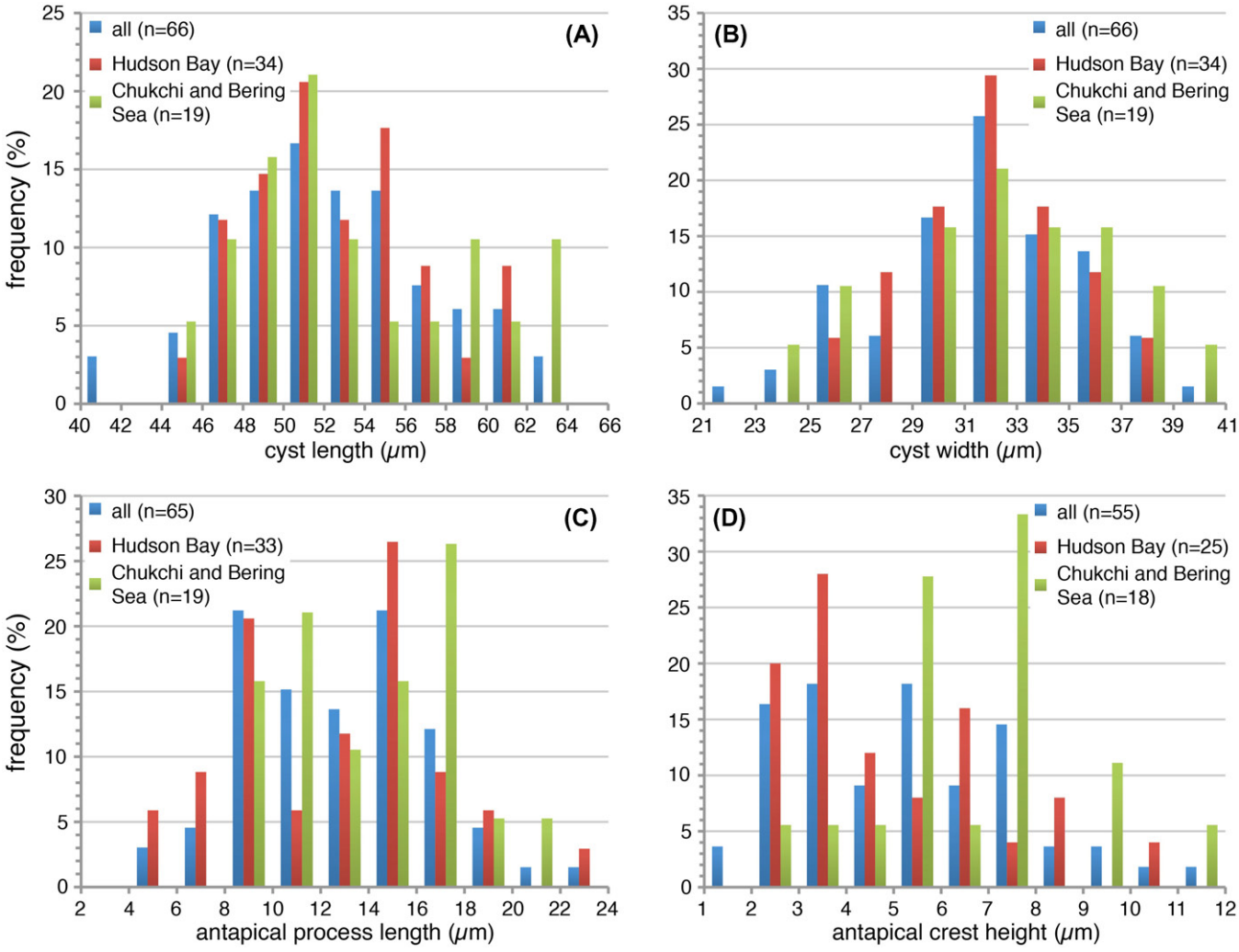


**Figure 6.** Frequency distribution diagram (A–C: 2 μm bins; D: 1 μm bins) for measured elongate *Spiniferites* cysts, for the total dataset (blue), cysts from Hudson Bay (red) and cysts from the Chukchi and Bering Sea (green). A) Cyst length; B) Cyst width; C) Antapical process length; D) Antapical crest height.

against a straight-forward, (semi-) quantitative relationship between cyst morphology and sea surface parameters. Furthermore, despite environmental resemblance to the Arctic shelf seas, the measurements from the Alaskan coast and Hudson Bay are not clearly separated from those of the more southern sites (Figures 1–5).

### 4.2. Beaufort Sea cyst sequences and relation to *Gonyaulax elongata*

The sequences obtained from the nine cysts isolated from surface sediments from the Beaufort Sea were variable in length, ranging from 2815 to 3612 nucleotides. They contained a portion of the SSU rDNA, the complete hypervariable ITS rDNA, and a portion of the LSU rDNA. The sequences were all identical, with the exception that the sequence of cyst E (KU358946) contained two locations within the ITS rDNA where the identification of the nucleotide was ambiguous. While different nucleotides were possible at these locations, the nucleotide present on all other sequences was part of the ambiguity. Therefore, this sequence was not differentiable from the sequences of other cysts. The variability in morphology of the wild cysts attributable to *Spiniferites elongatus* sensu lato from the Beaufort Sea was not reflected in the genetic analyses. The stability of the ITS rDNA between morphotypes attributable to *Spiniferites elongatus* sensu lato suggests that the morphological variability observed is intraspecific (Litaker et al. 2007) for the specimens of the Beaufort Sea and highlights the presence of such variability within *Spiniferites elongatus* sensu lato. Therefore, the genetic data in combination with the continuum that appears to exist between the extremes of the morphological spectrum suggest that morphotypes that correspond to the criteria describing *Spiniferites frigidus* and *Rottnestia amphicavata* should also be considered *Spiniferites elongatus* from a geological point of view, or cysts of *Gonyaulax elongata* from a biological point of view (also see section 5 below).

Only three out of 1348 nucleotides of the LSU rDNA (i.e. 0.2%) differentiated the Beaufort Sea cyst sequences from the sequence of *Gonyaulax elongata* of the Orkney Islands, Scotland, United Kingdom (Ellegaard et al. 2003). These differences are minor as reflected by the phylogenetic analyses that fully support (bootstrap value: 100%; posterior probability: 1.00) the relationship between *Gonyaulax elongata* from the United Kingdom and *Spiniferites*

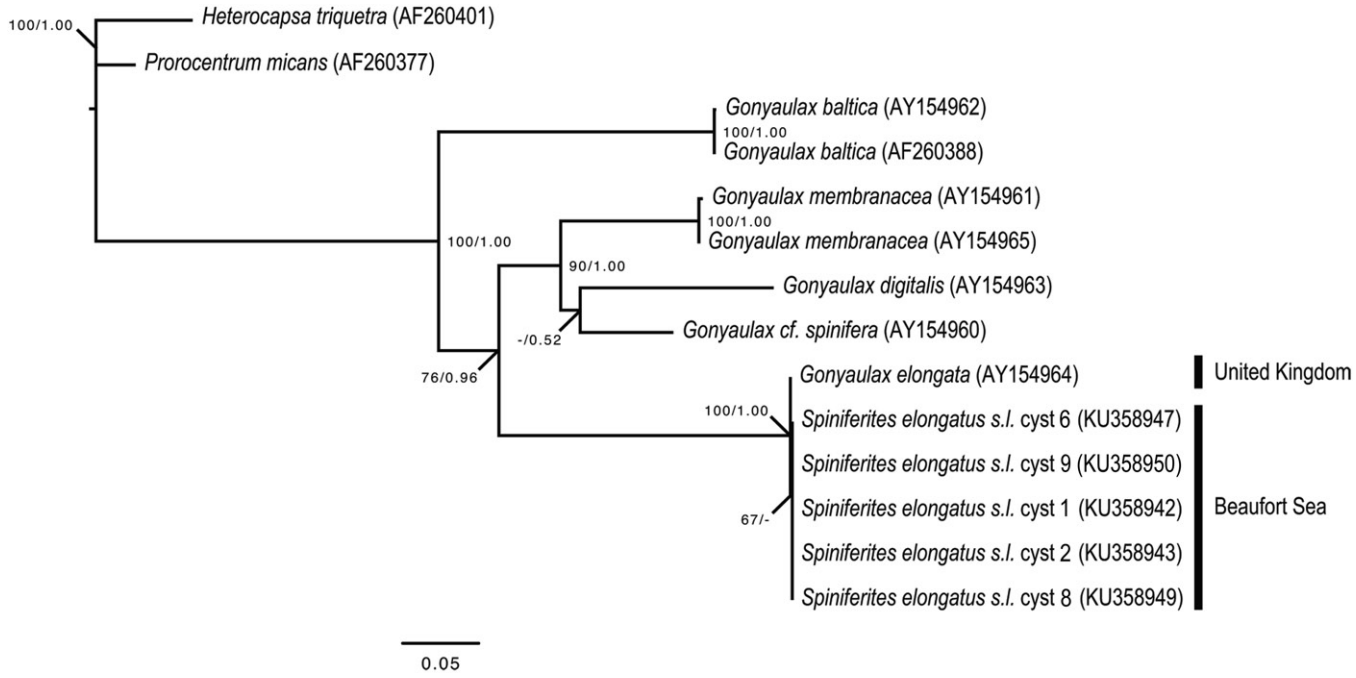


**Figure 7.** Maximum likelihood (ML) phylogenetic tree based on 799 aligned nucleotides of the nuclear large subunit ribosomal RNA (LSU rDNA) using the TIM3 + G model with *Heterocapsa triquetra* (Ehrenberg 1840) Stein 1883 and *Prorocentrum micans* as outgroup taxa. Alignment length includes gaps. The numbers at the nodes of the branches indicate the ML bootstrap (left) and Bayesian posterior probability (right) values; only values ≥50% or 0.5 are shown. Genbank accession numbers are provided.

*elongatus* sensu lato from the Beaufort Sea (Figure 7), and contrast with the long branches that separate different species within the genus *Gonyaulax* Diesing 1866 (Ellegaard et al. 2003; Mertens et al. 2015). The minor genetic differences observed between specimens of various locations might be representative of ecotypes within *Spiniferites elongatus* sensu lato. However, further analyses of specimens covering the global distribution of the species are required to conclude to the presence of genetically distinct geographic varieties and possibly cryptic diversity within *Spiniferites elongatus* sensu lato.

## 5. Systematic palaeontology

Division DINOFLAGELLATA (Bütschli 1885)
Fensome et al. 1993, emend. Adl et al. 2005
Class DINOPHYCEAE Pascher 1914
Subclass PERIDINIPHYCIDAE Fensome et al. 1993
Order GONYAULACALES Taylor 1980
Suborder Gonyaulacineae autonym
Family Gonyaulacaceae Lindemann 1928
Subfamily Gonyaulacoideae autonym
Genus *Spiniferites* Mantell 1850, emend. Sarjeant 1970

*Spiniferites elongatus* Reid 1974, emend. nov.
Plates 1–10

**Synonymy.** Resting spore of *Gonyaulax* sp. 1. Wall and Dale, 1968, pl. 1 fig. 16 [*fide* Reid 1974].

cf. *Hystrichosphaera* sp. a. Harland and Downie 1969, p. 232, pl. 7 fig. 4 [*fide* Reid 1974].

*Spiniferites ellipsoideus* Matsuoka 1983, p. 132–133, pl. 13 figs 6–7.

*Spiniferites frigidus* Harland and Reid in Harland et al. 1980, p. 213–216, fig. 2A–J.

*Rottnestia amphicavata* Dobell and Norris in Harland et al. 1980, p. 218–220, fig. 4A–N.

*Rottnestia amphicavata* var. B Dobell and Norris in Harland et al. 1980, p. 220–222, fig 4O–P, 8A–E, J–P.

*Rottnestia amphicavata* var. C Dobell and Norris in Harland et al. 1980, p. 222, fig. 8F–I, Q, R.

*Spiniferites* cf. *elongatus* Harland and Sharp 1986, pl. 1 figs 9–16.

**Motile affinity.** *Gonyaulax elongata* Ellegaard et al. 2003.

When the biological relationship between the cyst taxon *Spiniferites elongatus* and the then newly identified motile stage referred to as *Gonyaulax elongata* was revealed by Ellegaard et al. (2003), these authors proposed *Spiniferites elongatus* to be a basionym of the latter, and the cysts to be referred to as 'cyst of *Gonyaulax elongata*', following nomenclatural rules and scientific practice in place at that time. Indeed, the morphological and genetic observations made here and previously (Ellegaard et al. 2003) fully support the use of the taxonomic entity '*Gonyaulax elongata*' to refer to all life stages of this dinoflagellate in modern and sub-recent material. But while the modern relationship between the motile and cyst stage is unambiguous, it can be questioned whether this cyst–theca relationship goes all the way back to the Miocene, or if the cyst morphology has 'evolved' on one or several occasions – something that might be deduced from a detailed inspection (beyond the scope of this study) of the stratigraphic continuity of *Spiniferites elongatus* since its first appearance. Furthermore, in the appraisal of evolutionary pathways, it is important to stress that the genus *Gonyaulax* is not equivalent to the cyst-based genus

*Spiniferites*, since motile stages that are referred to as *Gonyaulax* are known to produce cysts that belong to other and different well-established fossil genera [e.g. *Gonyaulax digitale* (Pouchet 1883) Kofoid 1911 producing cysts known as *Bitectatodinium tepikiense* Wilson 1973 (Lewis et al. 2001); *Gonyaulax spinifera*-type dinoflagellates producing cyst morphologies attributable to *Spiniferites ramosus* (Ehrenberg 1837) Mantell 1854 sensu Rochon et al. 1999 and *Nematosphaeropsis labyrinthus* (Ostenfeld 1903) Reid 1974 (Rochon et al. 2009)]. Since its revision in 2011, article 11.1 of the International Code of Nomenclature for algae, fungi and plants stipulates that 'the use of separate names is allowed for fossil-taxa that represent different parts, life-history stages, or preservational states of what may have been a single organismal taxon … ' (McNeill et al. 2012). As such, both '*Spiniferites elongatus*' and 'cyst of *Gonyaulax elongata*' still are taxonomically valid designations of the cyst stage.

**Holotype, type stratum and locality.** Reid 1974, pl. 3, micrographs 23, 24. Surface sediment from the Estuary River Ythan, Scotland. See Gurdebeke et al. (2018) for new photomicrographs of the holotype.

**Original diagnosis.** 'Elongate ellipsoidal *Spiniferites* cysts ornamented by wide flaring sutural septae [sic]. Septae [sic] attached close to the centre of plate areas, the place of attachment appearing as an oval line on each plate. Septae [sic] varying in height from high complex processes at the antapex, high sutural flanges at the apex and low simple gonal processes in the girdle zone. Girdle displaced by its own width. Sulcus aligned parallel to the longitudinal axis increasing to three times its anterior width posteriorly' (Reid 1974, p. 602).

**Emended diagnosis.** Elongate *Spiniferites* cysts, appearing ellipsoidal in dorso-ventral view and circular in polar view. The exclusively gonal tapering processes are typically shorter in the cingular area and typically longer towards the antapex. Specimens with reduced processes can have them of about equal length. The processes are joined by claudate (i.e. distally closed) sutural septa of variable height, ranging from low rudimentary sutural crests to muri equally high as the adjoining process stems. The body wall is composed of two layers, and detachment of the tegillum (i.e. outer layer) from the pedium (i.e. inner layer) at the sutures causes suturocavation under the proximally hiate (i.e. open near to the cyst) septa. Extreme detachment of the tegillum and pedium at plate intersections in the apical and, particularly, antapical regions can induce circumcavation. In such case, this creates hollow process shafts that appear arch-like when seen in the optical section from a dorso-ventral view. The tegillum is smooth, very slightly uneven (shagreenate to scabrate) to microgranular; the pedium is smooth. Cingulum displaced by less than 1 to up to 2 times its own width, without overlap. Sulcus widens posteriorly. Saphopylic archaeopyle formed through the loss of plate 3″. The tabulation is consistent and typical gonyaulacacean, with the Kofoidian plate formula following the homologue approach: Po, 4′, 6″, 6c, 5 s, *6‴, 1p, 1⁗.

**Emended description.** The cyst has an elongated shape that is typically ellipsoidal, but it can appear more cylindriform especially in heavily ornamented and membranous specimens (e.g. Plate 3, figures 1–5). The cyst appears circular in polar view. SEM observations show that the paratabulation (Po, 4′, 6″, 6c, 5 s, *6‴, 1p, 1⁗) is of the standard gonyaulacacean type, with the first postcingular plate (1‴) absorbed in the sulcal plate series following the homologue approach (Fensome et al. 1993) (Plate 8; see also fig. 20 in Ellegaard et al. 2003). The sulcus widens towards the antapex, and plates as, ras, ls, rs, and ps are reflected to varying degrees but difficult to observe even under SEM (Plate 8). Often they are more clearly expressed when the crests are more elevated. There are four apical plates, with the suture between 1′ and 4′ often faint but (under SEM) always visible (Plate 7). Under SEM, the reflection of the ventral pore between 1′ and 4′ can be observed ('a' in Plate 7), and the apical pore complex is indicated by a single process with a swollen base ('b' in Plate 7). There are six precingular plates with 1″, 3″, 5″ 'penta' and 2″, 4″, 6″ 'quadra', with 6″ subtriangular, long and narrow (Plates 7–8). The six cingular plates are arranged as documented previously by Ellegaard et al. (2003) (Plates 8–9). The archaeopyle is reduced, saphopylic and formed through the loss of plate 3″ (e.g. Plate 9, figure 2). The height of the septa that connect the exclusively gonal processes can vary between specimens and on one individual. The septum height usually increases towards the processes, but can also be more or less equal all along the suture, giving those specimens a particularly membranous appearance. The highest septum is typically located at the junction of *4‴ and 1⁗. Similarly, the length of the processes varies, and they are usually shortest in the cingular area and longest at the antapex. The processes have trifurcate endings with more or less well-developed bifid tips, except for the processes located on the ventral antapical side which show different degrees of fusing of adjacent processes and hence multifurcate distal ends (Plate 10), and the process at the apex which is bifurcate (Plate 7). When the processes are short, their length is more uniform and the distal endings can be reduced to pointy or blunt, bulbous forks. In such cases of significant reduction of the processes, the bulbous endings appear to be sitting on top of the crests of the septa and are the only indication for the presence of processes (Plate 6). When the processes are long and well developed, the antapical processes can appear subconical rather than tapering, and somewhat trumpet shaped at 1p/*3‴/1⁗ and *5‴/*6‴/1⁗. Both the dorsal and ventral antapical processes can be hollow and open distally, with tiny perforations or large openings, depending on the elevation of hollow sutures (Plate 10; see also figs 23 and 27 in Ellegaard et al. 2003). The wall is composed of two layers, and cavation occurs through the detachment of the pedium (i.e. inner layer) and the tegillum (i.e. outer layer) at both the plate sutures and triple junctions (e.g. Plate 2, figure 6). The penitabular contact between the pedium and tegillum is often readily seen as a discrete line on several plates and gives the latter a rounded appearance. The contact can be very close to the sutures, resulting in only little suturocavation and

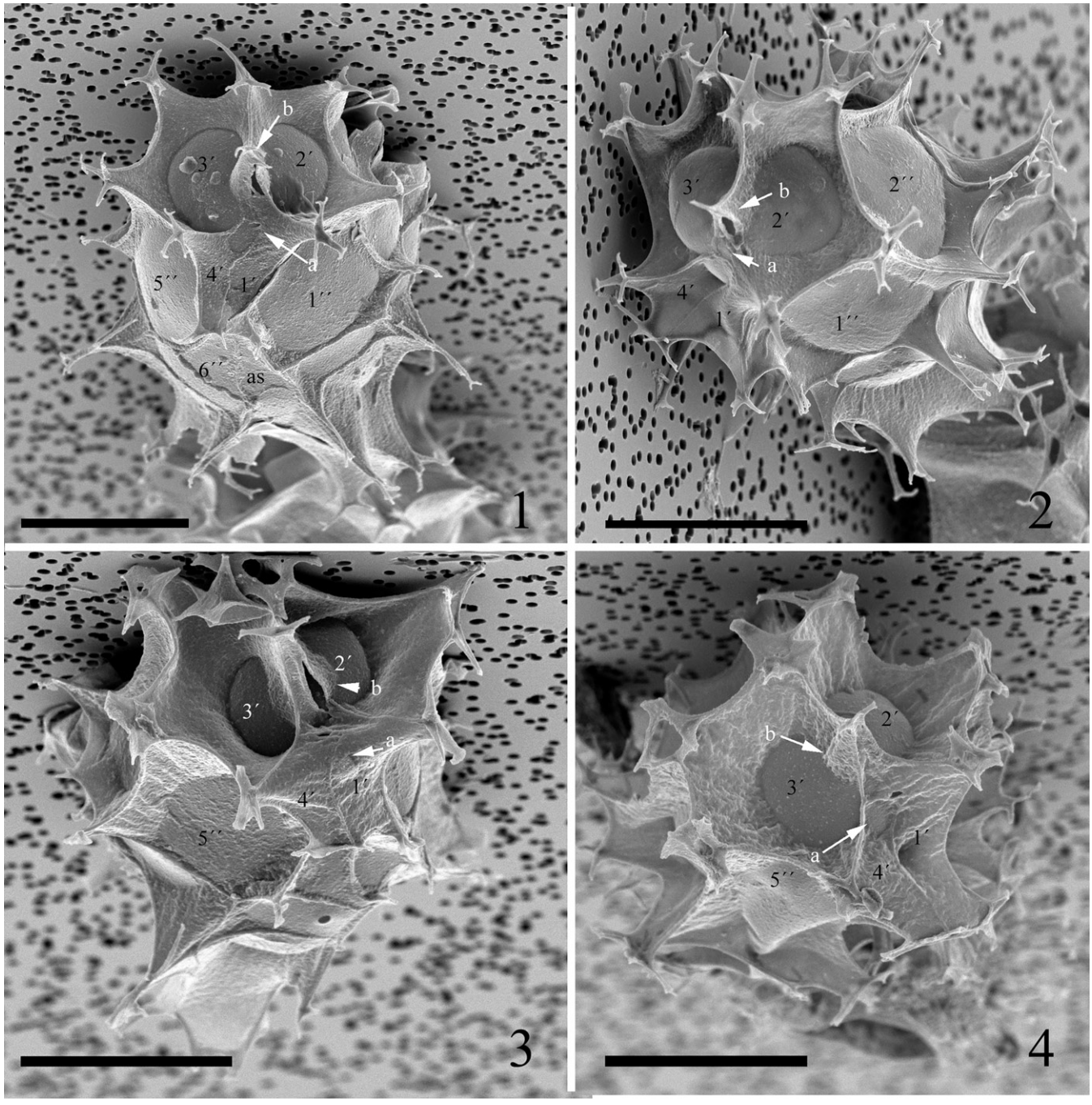


**Plate 7.** 1–4. Scanning electron micrographs of apical views of four different specimens of *Spiniferites elongatus* from the Barents Sea with significant variation in the elevation of sutural crests, all showing consistently four apical plates (1′–4′). Note a faint suture between 1′ and 4′. 'a' indicates reflection of ventral pore; 'b' indicates reflection of apical pore. as = anterior sulcal plate. Scale bars = 10 μm.

apparently more rigid septa, or can be located farther towards the interior of the plates, resulting in an elaborate drape-like appearance (Plates 7–10). Very pronounced cavation can occur apically under the process and, particularly, antapically along the 1p/1′′′′, *3′′′/1′′′′ and *5′′′/1′′′′ sutures. Occasionally the cavation also includes the 1p/*3′′′ and *6′′′/1′′′′, or even up to the *2′′′/*3′′′ sutures (see, for instance, fig. 2J in Harland et al. 1980). When seen in optical section, the pronounced antapical cavities formed in this way can be equal or different in size, and look like an inverted, open arch (e.g. Plate 5, figure 4). The tegillum and pedium always stay in contact near the middle of plate 1′′′′.

**Dimensions.** Holotype: body width 30 μm and length 49 μm; antapical process length 13 μm; apical process length 6 μm; lateral process length 9 μm. Topotypes: 15 specimens measured by Reid (1974): range of body width 26–40 μm; range of body length 42–59 μm; antapical process length 12–16 μm; apical process length 6–12 μm; lateral process length 5–9 μm. Ranges from this study: body length 42 (53) 64 μm, body width 23 (32) 41 μm, 66 specimens measured; antapical process length 5 (13) 22 μm, 65 specimens measured; antapical crest height, 2 (6) 12 μm, 55 specimens measured. See also Table 2.

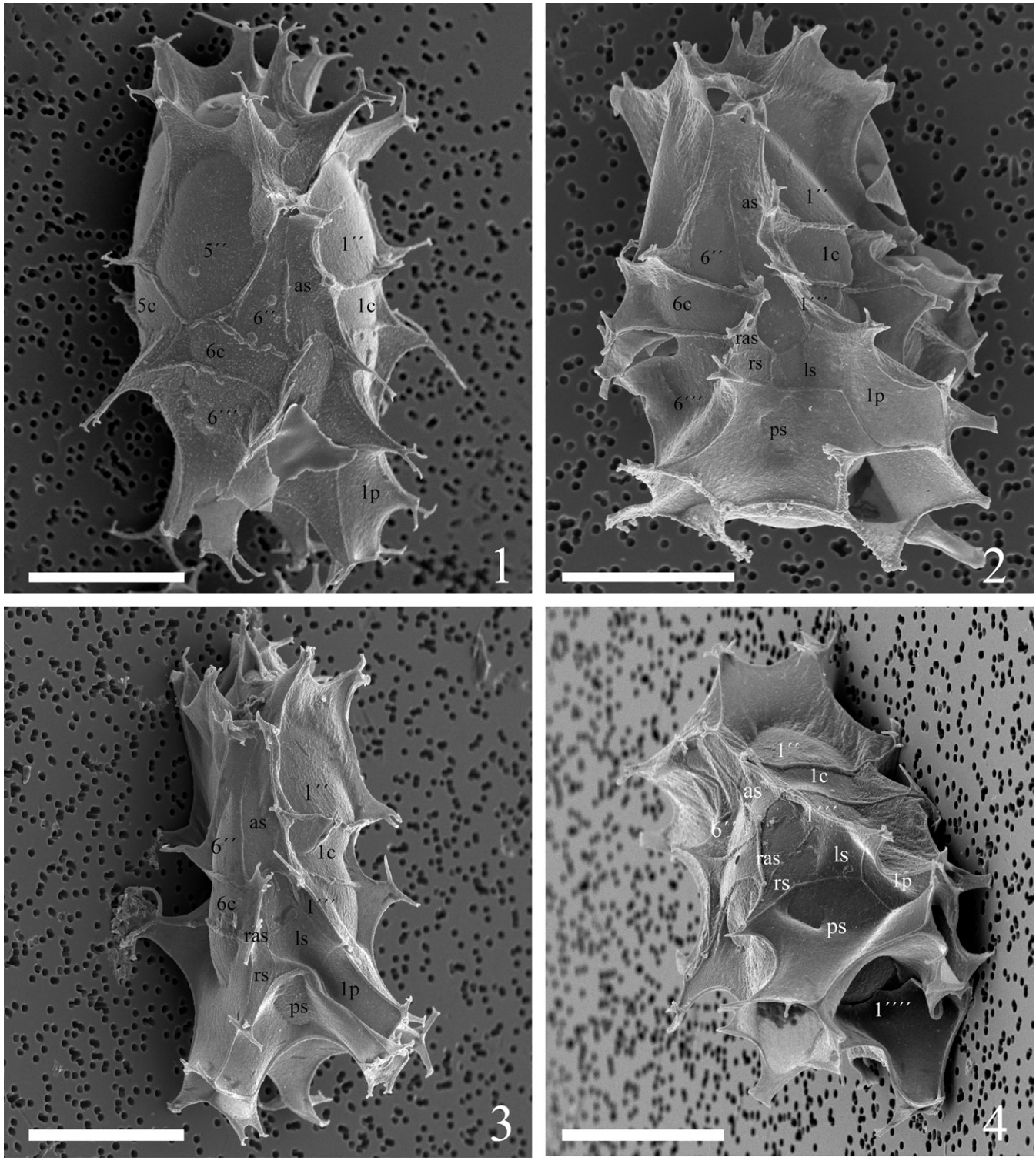


**Plate 8.** 1–4. Scanning electron micrographs of ventral views of four different specimens of *Spiniferites elongatus* from the Barents Sea with significant variation in the elevation of sutural crests, all showing the same displacement of one cingular width and configuration of sulcal plates. 1p = posterior intercalary plate, as = anterior sulcal plate, ls = left sulcal plate, ps = posterior sulcal plate, ras = right accessory plate, rs = right sulcal plate. Scale bars = 10 μm.

**Comparison.** Specimens where the processes are short and strongly reduced, or nearly completely integrated into the high sutural septa, might appear similar to some *Impagidinium* Stover and Evitt 1978 species (e.g. *Impagidinium aculeatum* (Wall 1967) Lentin and Williams 1981), but can be distinguished from the latter by the pointy or blunt distal process terminations sitting on top of the crests of the septa and indicating the presence of processes in such *Spiniferites elongatus* specimens (e.g. Plate 3, figure 8, and Plate 6).

**Remarks with respect to the original descriptions.** The presence of a slight apical boss was mentioned for *Spiniferites frigidus* by R. Harland and P.C. Reid (in Harland et al. 1980) but was not seen in any of the specimens observed by the authors of the present paper. Even though

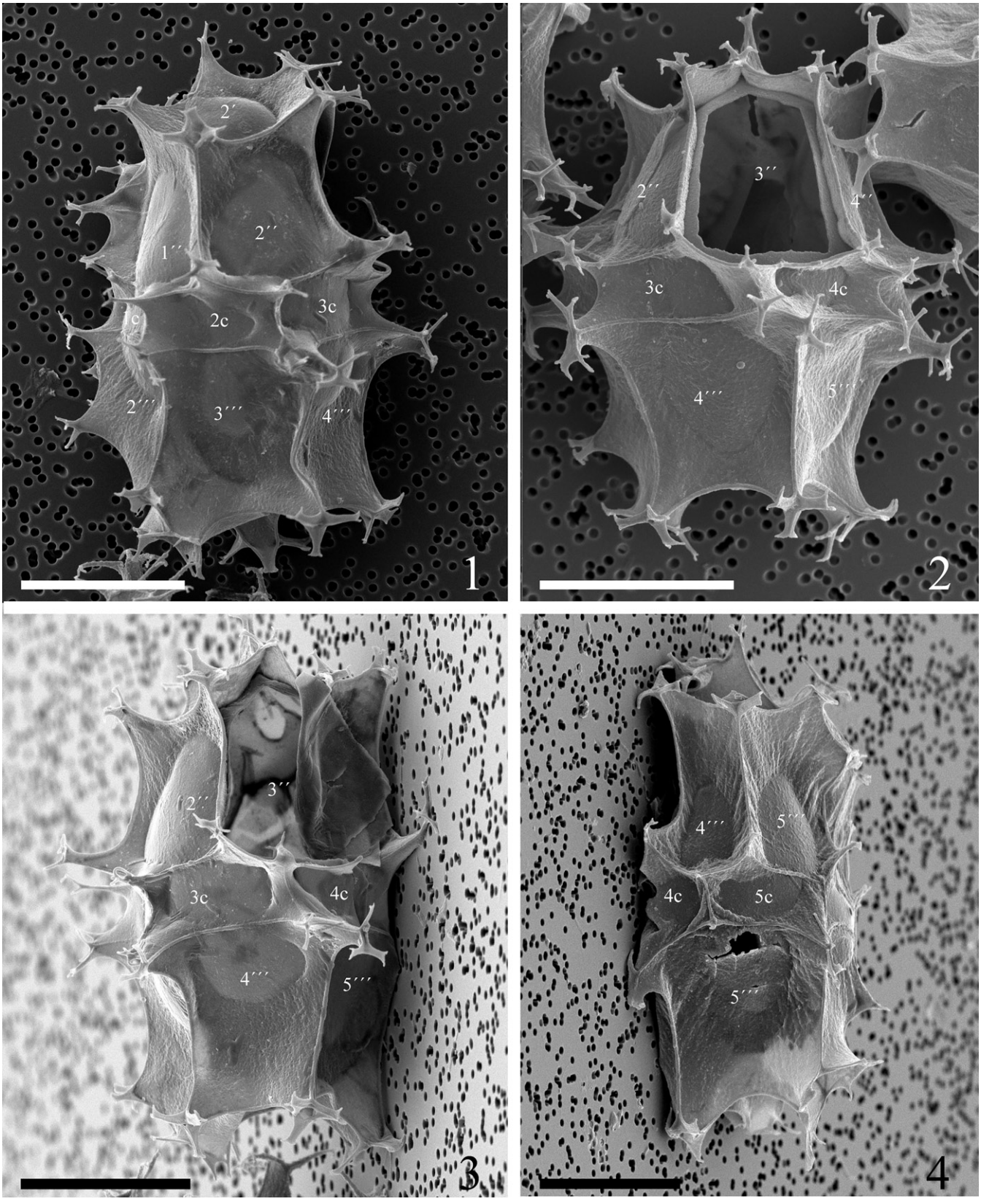


**Plate 9.** 1–4. Scanning electron micrographs of lateral and dorsal views of four different specimens of *Spiniferites elongatus* from the Barents Sea with significant variation in the elevation of sutural crests, showing the position of sulcal plate boundaries and a reduced archaeopyle corresponding to 3′′. Scale bars = 10 μm.

it was not explicitly stated in the original description of *Spiniferites elongatus* (Reid 1974), the processes on this species appear to be exclusively gonal. The presence of 'strengthening rods that appear to support the multifurcate [process] tips' (Reid 1974, p. 603) cannot be confirmed by our observations. It should be further noted that only since the revision of the Kofoidian tabulation by Evitt (1985) did the gonyaulacoid concept with six postcingular plates, with

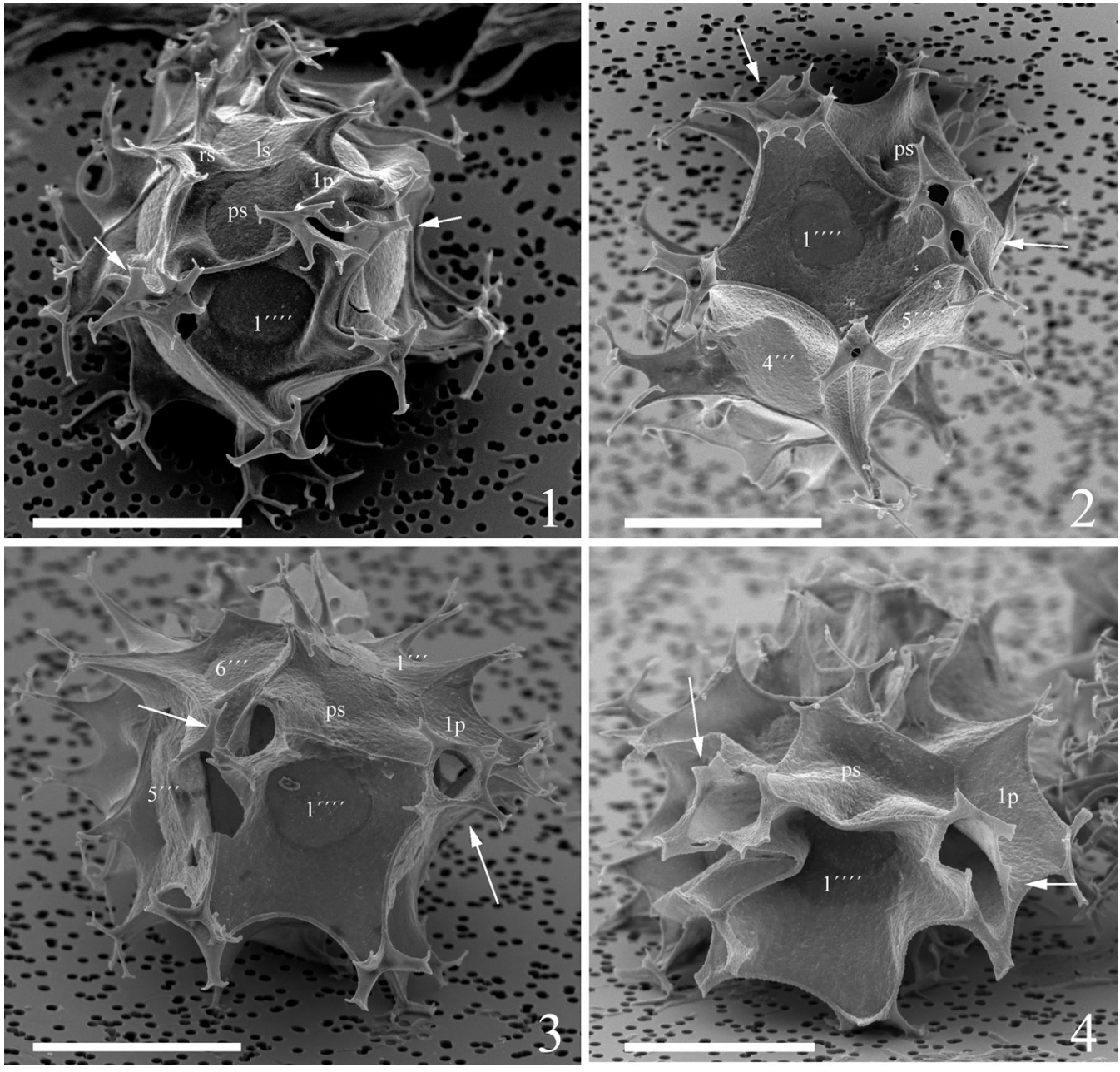


**Plate 10.** 1–4. Scanning electron micrographs of antapical views of four different specimens of *Spiniferites elongatus* from the Barents Sea with significant variation in the elevation of sutural crests, showing the antapical plate configuration with significant variation in fusion of ventral antapical multifurcate processes, indicated by white arrows on all specimens. 1p = posterior intercalary plate, ls = left sulcal plate, ps = posterior sulcal plate, rs = right sulcal plate. Scale bars = 10 μm.

the first postcingular plate often incorporated into the sulcus, become established. This is indeed the case for *Spiniferites elongatus* (Plate 8; Ellegaard et al. 2003, their fig. 20) and therefore the designated number of each of the postcingular plates identified by Reid (1974) should be 'shifted' one number up. Thus, the plates that were originally named 2′′′, 3′′′, 4′′′ and 5′′′ are now referred to as *3′′′, *4′′′, *5′′′ and *6′′′ following the Kofoidian tabulation system. Consequently, the two hollow trumpet-shaped processes observed by Reid (1974) are located at *6′′′/*5′′′/1′′′′ and 1p/*3′′′/1′′′′, while the 'high membranous septae [sic] joining two stout simple processes' (Reid 1974, p. 603) is situated at the junction of plates *4′′′ and 1′′′′ (Plate 10; see also figs 20, 21, 23 and 24 in Ellegaard et al. 2003).

**Discussion.** When the elongate species *Spiniferites ellipsoideus* was originally described, it was differentiated from *Spiniferites elongatus* based on its shorter and wider cyst body (Matsuoka 1983). However, this distinguishing criterion is no longer tenable given the considerable size overlap between the type population of *Spiniferites ellipsoideus* and modern populations of *Spiniferites elongatus*. Hence, *Spiniferites ellipsoideus* has to be considered a junior synonym of *Spiniferites elongatus*, as suspected earlier by Williams et al. (1993, p. 23). The Late Oligocene to Early Miocene species *Rottnestia ovata* Matsuoka and Bujak 1988 also has an elongate, albeit slightly more oval, body shape and was distinguished from *Spiniferites ellipsoideus* by the more conspicuous apical and antapical pericoels in *Rottnestia ovata*

(Matsuoka and Bujak 1988). Based on the data currently at hand, *Rottnestia ovata* is not considered to be conspecific with *Spiniferites ellipsoideus* and, thus, *Spiniferites elongatus*. Arguably, *Rottnestia ovata* might represent an ancestral form of *Spiniferites elongatus*.

As mentioned in section 2.1, Dobell and Norris (in Harland et al. 1980) assigned *Rottnestia amphicavata* to the genus *Rottnestia* based on the presence of apical and antapical pericoels, but at the same time they also assigned varieties lacking these pericoels to the genus, leaving some confusion about their application and interpretation of a pericoel as criterion to justify this assignment.

Strictly speaking, cavities that result from spot detachment between the pedium and tegillum under the bases of processes or sutural features constitute pericoels. However, as applied in the original description of *Rottnestia* and its type species *Rottnestia borussica* (Eisenack 1954) Cookson and Eisenack 1961, both the apical and antapical pericoels extend across the entire plate(s). Thus, cysts belonging to *Rottnestia* are typically bicavate, with the tegillum completely detached from the pedium in the apical and antapical area. This does not seem to be the case in *amphicavata*: here, the apical pericoel 'occurs under the process which is present at the junction of plates 1′, 2′ and 3′′ … ' (Dobell and Norris in Harland et al. 1980, p. 219), and the tegillum stays in contact with the pedium in the middle of plate 1′′′′, i.e. at the site of the 'funnel-like invagination of the periphragm' (Dobell and Norris in Harland et al. 1980, p. 219) (cf. Plate 1, figure 8, Plate 4, figure 7 and Plate 5, figure 4). As such, the 'hydropyles', interpreted by Dobell and Norris to connect the pericoel to the exterior through an opening in the processes, do not represent openings but the triple junction of the septa at *3′′′/*4′′′/1′′′′ (on the left side of the cyst) and *4′′′/*5′′′/1′′′′ (not *2′′′/*3′′′/1′′′′ as originally identified, on the right side of the cyst). Thus, the apical and antapical cavities represent well-developed suturocavations that are restricted to the sutural area; they do not represent true pericoels as used in the definition of *Rottnestia*. Adding the absence in *Rottnestia amphicavata* of an apical cylindrical or conical horn ascribed to the genus (Cookson and Eisenack 1961), the above reasoning argues against the generic attribution to *Rottnestia* on the basis of the nature of the cavation in these morphologies, which can be accommodated in *Spiniferites* (cf. Evitt 1985, p. 228). Further taking into account the morphological continuum between typical *Spiniferites elongatus* (sensu Reid 1974) and morphotypes ascribed to *Spiniferites frigidus* and *Rottnestia amphicavata*, the latter two species are considered junior synonyms to *Spiniferites elongatus*. Consequently, we also argue that cysts that have been identified as *Rottnestia amphicavata* possess four apical plates, and that this could not be observed clearly in earlier studies because of the high sutural septa in combination with the often very faint appearance of the suture between 1′ and 4′ (see above).

## 6. Taxonomic implications and recommendations

Based on the results presented here, we make the following suggestions:

(1) The *amphicavata* morphology does not conform to the generic criteria that define *Rottnestia*, and its morphological characteristics represent the extreme end in a continuum from 'typical' *Spiniferites elongatus* (sensu Reid 1974) towards more pronounced septal development and circum-suturocavation. Those extreme features can be accommodated in the genus *Spiniferites* and are expressions of the intraspecific variability within *Spiniferites elongatus*, as supported by the molecular data. Consequently, we consider *Rottnestia amphicavata* and *Spiniferites frigidus* to be conspecific – as already suggested by Bujak (1984) – and these two morphological variants as junior synonyms of *Spiniferites elongatus*.

(2) The morphological measurements fail to establish a significant relation between the morphology of *Spiniferites elongatus* sensu lato and environmental conditions. However, as limited quantitative data are currently available, we recommend the use in palaeoenvironmental studies of two informal cyst types along with *Spiniferites elongatus* sensu stricto to differentiate specimens situated at the extreme ends of the morphological spectrum. The first suggested type, to be referred to as '*Spiniferites elongatus* – Norwegian morphotype', includes specimens with strongly reduced processes bearing short, blunt terminations that sometimes simply seem to sit on top of the sutural septa and as such are the only indication of the presence of processes (e.g. Plate 6). This type includes the specimens first described from the Norwegian Sea by Harland and Sharp (1986) and referred to by them as *Spiniferites* cf. *elongatus*. The second type, '*Spiniferites elongatus* – Beaufort morphotype', distinguishes the more flamboyant forms with strongly developed sutural septa from typical *Spiniferites elongatus* cysts, and refers to the morphological features first encountered in specimens from Beaufort Sea surface sediments that led to the description of *Spiniferites frigidus* and *Rottnestia amphicavata* by Harland et al. (1980). However, the morphological continuum makes it difficult to define a clear cut-off criterion for the *Spiniferites elongatus* – Beaufort morphotype. To reduce observer bias, we suggest the invagination of the antapical crest in between the antapical processes as a semi-quantitative tool in the assessment of the overall 'flanginess' of a specimen; thus, specimens with long antapical processes can be identified as *Spiniferites elongatus* – Beaufort morphotype when the antapical crest height exceeds half the length of the antapical processes.

(3) Census analyses should ideally be combined with morphometric analyses, for instance through the measuring of cyst width and length, antapical process length, and the height of the apical and antapical membranes. Eventually, this type of data could be used to establish, or refute the existence of, a (semi-)quantitative relation between cyst morphology and sea surface parameters.

## Acknowledgements

We acknowledge fruitful discussions with, and input from, Laurent Londeix, Claus Heilmann-Clausen, André Rochon and Martin Head on the taxonomical concepts of *Spiniferites* and *Rottnestia*. Kazumi Matsuoka kindly provided new photographs of the holotype of *Spiniferites* '*ellipsoideus*'. We thank Nicolas Gayet for the use of microscope facilities

at Ifremer Brest. We also thank Drs Robie W. Macdonald (Institute of Ocean Sciences, Department of Fisheries and Oceans, Canada), Gary A. Stern (University of Manitoba, Canada), Louis Fortier (Université Laval, Canada), and Charles Gobeil (Institut National de la Recherche Scientifique, Canada) for providing some sediment samples.

## Disclosure statement

No potential conflict of interest was reported by the authors.

## Funding

Funding to NVN was provided by the Danish Council for Independent Research, Natural Science [project no. 12–126709/FNU]. The genetic work by EP was supported by the K-PORT [Korea-Polar Ocean in Rapid Transition, KOPRI, PM15040] and K-POD [Korea-Polar Ocean Development, KOPRI, PM15050] projects funded by the Ministry of Oceans and Fisheries of Korea. This research was partially funded by the Natural Sciences and Engineering Research Council of Canada (NSERC) through a Discovery grant to VP. She is the Hanse-Wissenschaftskolleg (HWK) senior research fellow in marine and climate research at the Institute for Advanced Study (Germany). Funding for MH was provided by the Academy of Finland [grant 252512] and the Villlum Foundation, Denmark [VKR 023454].

## References

Adl SM, Simpson AGB, Farmer MA, Andersen RA, Anderson OR, Barta JR, Bowser SS, Brugerolle G, Fensome RA, Fredericq S. 2005. The new higher level classification of Eukaryotes with emphasis on the taxonomy of Protists. J Eukaryot Microbiol. 52(5):399–451.

Bolch CJS. 2001. PCR protocols for genetic identification of dinoflagellates directly from single cysts and plankton cells. Phycologia. 40(2): 162–167.

Bujak JP. 1984. Cenozoic dinoflagellate cysts and acritarchs from the Bering Sea and northern North Pacific, DSDP Leg 19. Micropaleontology. 30(2):180–212.

Cookson IC, Eisenack A. 1961. Tertiary microplankton from the Rottnest Island Bore, Western Australia. J Royal Soc West Aus. 44:39–47.

Darriba D, Taboada GL, Doallo R, Posada D. 2012. jModelTest 2: more models, new heuristics and parallel computing. Nat Methods. 9(8): 772.

Daugbjerg N, Hansen G, Larsen J, Moestrup Ø. 2000. Phylogeny of some of the major genera of dinoflagellates based on ultrastructure and partial LSU rDNA sequence data, including the erection of three new genera of unarmoured dinoflagellates. Phycologia. 39(4):302–317.

de Vernal A, Henry M, Matthiessen J, Mudie PJ, Rochon A, Boessenkool K, Eynaud F, Grøsfjeld K, Guiot J, Hamel D, et al. 2001. Dinoflagellate cyst assemblages as tracers of sea-surface conditions in the northern North Atlantic, Arctic and sub-Arctic seas: the new 'n = 677' database and application for quantitative paleoceanographical reconstruction. J Quat Sci. 16(6):3–699.

de Vernal A, Eynaud F, Henry M, Hillaire-Marcel C, Londeix L, Mangin S, Matthiessen J, Marret F, Radi T, Rochon A, et al. 2005. Reconstruction of sea-surface conditions at middle to high latitudes of the Northern Hemisphere during the Last Glacial Maximum (LGM) based on dinoflagellate cyst assemblages. Quat Sci Rev. 24(7–9):897–924.

de Vernal A, Rochon A, Fréchette B, Henry M, Radi T, Solignac S. 2013. Reconstructing past sea ice cover of the Northern Hemisphere from dinocyst assemblages: status of the approach. Quat Sci Rev. 79: 122–134.

de Vernal A, Eyaud F, Henry M, Limoges A, Londeix L, Matthiessen J, Marret F, Pospelova V, Radi T, Rochon A, et al. 2018. Distribution and (palaeo)ecological affinities of the main Spiniferites taxa in the mid-high latitudes of the Northern Hemisphere. Palynology. doi:10.1080/01916122.2018.1465730

Eisenack A. 1954. Mikrofossilien aus Phosphoriten des samländischen Unteroligozäns und über die Einheitlichkeit der Hystrichosphaerideen. Palaeontographica, Abteilung A. 105:49–95.

Ellegaard M. 2000. Variations in dinoflagellate cyst morphology under conditions of changing salinity during the last 2000 years in the Limfjord, Denmark. Rev Palaeobot Palynol. 109(1):65–81.

Ellegaard M, Daugbjerg N, Rochon A, Lewis J, Harding I. 2003. Morphological and LSU rDNA sequence variation within the Gonyaulax spinifera-Spiniferites group (Dinophyceae) and proposal of G. elongata comb. nov. and G. membranacea comb. nov. Phycologia. 42(2):151–164.

Evitt WR. 1985. Sporopollenin dinoflagellate cysts: their morphology and interpretation. AASP Monograph Series. 1:333.

Fensome RA, Taylor FJR, Norris G, Sarjean WAS, Wharton DI, Williams GL. 1993. A classification of living and fossil dinoflagellates. Micropaleontology. Special Publication 7:1–351.

Fensome RA, MacRae RA, Williams GL. 2008. DINOFLAJ2, Version 1. American Association of Stratigraphic Palynologists, Data Series no. 1.

Gu H, Liu T, Mertens KN. 2015. Cyst-theca relationship and phylogenetic positions of Protoperidinium (Peridiniales, Dinophyceae) species of the sections Conica and Tabulata, with description of Protoperidinium shanghaiense sp. nov. Phycologia. 54(1):49–66.

Guindon S, Dufayard J-F, Lefort V, Anisimova M, Hordijk W, Gascuel O. 2010. New algorithms and methods to estimate maximum-likelihood phylogenies: assessing the performance of PhyML 3.0. Syst Biol. 59(3): 307–321.

Gurdebeke P, Mertens KN, Bogus K, Marret-Davies F, Vrielinck H, Louwye S. 2018. Taxonomic reinvestigation and geochemical characterization of Reid's (1974) species of Spiniferites from holotype and topotype material. Palynology. doi:10.1080/01916122.2018.1465735

Hall TA. 1999. BioEdit: a user-friendly biological sequence alignment editor and analysis program for Windows 95/98/NT. Nucleic Acids Symp Series. 41:95–98.

Harland R, Downie C. 1969. The dinoflagellates of the Interglacial Deposits at Kirmington, Lincolnshire. Proceedings of the Yorkshire Geol Soc. 37(2):231–237.

Harland R, Reid PC, Dobell P, Norris G. 1980. Recent and sub-Recent dinoflagellate cysts from the Beaufort Sea, Canadian Arctic. Grana. 19(3):211–225.

Harland R. 1982. Recent dinoflagellate cyst assemblages from the southern Barents Sea. Palynology. 6(1):9–18.

Harland R. 1983. Distribution maps of Recent dinoflagellate cysts in bottom sediments from the North Atlantic Ocean and adjacent seas. Palaeontology. 26:321–387.

Harland R, Sharp J. 1986. Elongate Spiniferites cysts from North Atlantic bottom sediments. Palynology. 10(1):25–34.

Heikkilä M, Pospelova V, Hochheim KP, Kuzyk ZZA, Stern GA, Barber DG, Macdonald RW. 2014. Surface sediment dinoflagellate cysts from the Hudson Bay system and their relation to freshwater and nutrient cycling. Marine Micropaleontology. 106:79–109.

Heikkilä M, Pospelova V, Forest A, Stern GA, Fortier L, MacDonald RW. 2016. Dinoflagellate cyst production over an annual cycle in seasonally ice-covered Hudson Bay. Marine Micropaleontology. 125:1–24.

Horiguchi T, Yoshizawa-Ebata J, Nakayama T. 2000. Halostylodinium arenarium, gen. et sp. nov. (Dinophyceae), a coccoid sand-dwelling dinoflagellate from subtropical Japan. J Phycol. 36(5):960–971.

Jansson I-M, Mertens KN, Head MJ, de Vernal A, Londeix L, Marret F, Matthiessen J, Sangiorgi F. 2014. Statistically assessing the correlation between salinity and morphology in cysts produced by the dinoflagellate Protoceratium reticulatum from surface sediments of the North Atlantic Ocean, Mediterranean–Marmara–Black Sea region, and Baltic–Kattegat–Skagerrak estuarine system. Palaeogeogr Palaeoclimatol Palaeoecol. 399:202–213.

Kawami H, van Wezel R, Koeman RPT, Matsuoka K. 2009. Protoperidinium tricingulatum sp. nov. (Dinophyceae), a new motile form of a round, brown, and spiny dinoflagellate cyst. Phycol Res. 57(4):259–267.

Kurita H, Ishikawa Y. 2009. Dinoflagellate cysts during the Middle Miocene Climatic Optimum (MMCO) from the Namiishi-zawa section

of the Kamagui Formation, northern Niigata, central Japan. Scientific Reports of the Niigata University. Geology. 24:63–79.
Larkin MA, Blackshields G, Brown NP, Chenna R, McGettigan PA, McWilliam H, Valentin F, Wallace IM, Wilm A, Lopez R, et al. 2007. Clustal W and Clustal X version 2.0. Bioinformatics. 23(21):2947–2948.
Lenaers G, Maroteaux L, Michot B, Herzog M. 1989. Dinoflagellates in evolution. A molecular phylogenetic analysis of large subunit ribosomal RNA. J Mol Evol. 29(1):40–51.
Lewis J, Rochon A, Ellegaard M, Mudie PJ, Harding I. 2001. The cyst-theca relationship of Bitectatodinium tepikiense (Dinophyceae). Euro J Phycol. 36(2):137–146.
Litaker RW, Vandersea MW, Kibler SR, Reece KS, Stokes NA, Steidinger KA, Millie DF, Bendis BJ, Pigg RJ, Tester PA. 2003. Identification of Pfiesteria piscicida (Dinophyceae) and Pfiesteria-like organisms using internal transcribed spacer-specific PCR assays. J Phycol. 39(s1): 36–761.
Litaker RW, Vandersea MW, Kibler SR, Reece KS, Stokes NA, Lutzoni FM, Yonish BA, West MA, Black MND, Tester PA. 2007. Recognizing dinoflagellate species using ITS rDNA sequences. J Phycol. 43(2):344–355.
Marret F, Zonneveld KAF. 2003. Atlas of modern organic-walled dinoflagellate cyst distribution. Rev Palaeobot Palynol. 125(1–2):1–200.
Matsuoka K. 1983. Late Cenozoic dinoflagellates and acritarchs in the Niigata district, central Japan. Palaeontogr Abteilung B. 187:89–154.
Matsuoka K, Bujak JP. 1988. Cenozoic dinoflagellate cysts from the Navarin Basin, Norton Sound and St. George Basin, Bering Sea. Bulletin of the Faculty of Liberal Arts, Nagasaki University. Nat Sci. 29: 1–147.
Matsuoka K, Bujak JP, Shimazaki T. 1987. Late Cenozoic dinoflagellate cyst biostratigraphy from the west coast of northern Japan. Micropaleontology. 33(3):214–229.
Matsuoka K, Kawami H, Fujii R, Iwataki M. 2006. Further examination of the cyst-theca relationship of Protoperidinium thulesense (Peridiniales, Dinophyceae) and the phylogenetic significance of round brown cysts. Phycologia. 45(6):632–641.
Matsuoka K, Kawami H, Nagai S, Iwataki M, Takayama H. 2009. Re-examination of cyst-motile relationships of Polykrikos kofoidii Chatton and Polykrikos schwartzii Bütschli (Gymnodiniales, Dinophyceae). Rev Palaeobot Palynol. 154(1–4):79–90.
McNeill J, Barrie FR, Buck WR, Demoulin V, Greuter W, Hawksworth DL, Herendeen PS, Knapp S, Marhold K, Prado J, et al. 2012. International Code of Nomenclature for algae, fungi and plants (Melbourne Code) adopted by the Eighteenth International Botanical Congress Melbourne, Australia, July 2011. Regnum Vegetabile.154. Koeltz Scientific Books, Oberreifenberg, Germany:240. pp.
Medlin L, Elwood HJ, Stickel S, Sogin ML. 1988. The characterization of enzymatically amplified eukaryotic 16S-like rRNA-coding regions. Gene. 71(2):491–499.
Mertens KN, Ribeiro S, Bouimetarhan I, Caner H, Combourieu Nebout N, Dale B, De Vernal A, Ellegaard M, Filipova M, Godhe A, et al. 2009. Process length variation in cysts of a dinoflagellate, Lingulodinium machaerophorum, in surface sediments: Investigating its potential as salinity proxy. Marine Micropaleontol. 70(1–2):54–69.
Mertens KN, Dale B, Ellegaard M, Jansson I-M, Godhe A, Kremp A, Louwye S. 2011. Process length variation in cysts of the dinoflagellate Protoceratium reticulatum, from surface sediments of the Baltic-Kattegat-Skagerrak estuarine system: a regional salinity proxy. Boreas. 40(2):242–255.
Mertens KN, Bringué M, Van Nieuwenhove N, Takano Y, Pospelova V, Rochon A, de Vernal A, Radi T, Dale B, Patterson RT, et al. 2012. Process length variation of the cyst of the dinoflagellate Protoceratium reticulatum in the North Pacific and Baltic-Skagerrak region: calibration as an annual density proxy and first evidence of pseudo-cryptic speciation. J Quat Sci. 27(7):734–744.
Mertens KN, Yamaguchi A, Kawami H, Ribeiro S, Leander BS, Price AM, Pospelova V, Ellegaard M, Matsuoka K. 2012. Archaeperidinium saanichi sp. nov.: a new species based on morphological variation of cyst and theca within the Archaeperidinium minutum Jörgensen 1912 species complex. Marine Micropaleontol. 96–97:48–62.
Mertens KN, Yamaguchi A, Takano Y, Pospelova V, Head MJ, Radi T, Pieńkowski AJ, de Vernal A, Kawami H, Matsuoka K. 2013. A new heterotrophic dinoflagellate from the North-eastern Pacific, Protoperidinium fukuyoi: cyst-theca relationship, Phylogeny, Distribution and Ecology. J Eukaryot Microbiol. 60(6):545–563.
Mertens KN, Aydin H, Uzar S, Takano Y, Yamaguchi A, Matsuoka K. 2015. Relationship between the dinoflagellate cyst Spiniferites pachydermus and Gonyaulax ellegaardiae sp. nov. from Izmir Bay, Turkey, and molecular characterization. J Phycol. 51(3):560–573.
Pospelova V, Chmura GL, Walker HA. 2004. Environmental factors influencing spatial distribution of dinoflagellate cyst assemblages in shallow lagoons of southern New England (USA). Rev Palaeobot Palynol. 128(1–2):7–34.
Pospelova V, Pedersen TF, de Vernal A. 2006. Dinoflagellate cysts as indicators of climatic and oceanographic changes during the past 40 kyr in the Santa Barbara Basin, southern California. Paleoceanogr. 21(2): 1–16. DOI:doi:10.1029/2005PA001251.
Reid PC. 1974. Gonyaulacacean dinoflagellate cysts from the British Isles. Nova Hedwigia. 25:579–637.
Rochon A, Lewis J, Ellegaard M, Harding I. 2009. The Gonyaulax spinifera (Dinophyceae) "complex": Perpetuating the paradox? Rev Palaeobot Palynol. 155(1–2):52–60.
Ronquist F, Huelsenbeck JP. 2003. MrBayes 3: Bayesian phylogenetic inference under mixed models. Bioinformatics. 19(12):1572–1574.
Sarjeant WAS. 1970. The genus Spiniferites Mantell, 1850 (Dinophyceae). Grana. 10(1):74–78.
Sildever S, Andersen J, Ribeiro S, Ellegaard M. 2015. Influence of surface salinity gradient on dinoflagellate cyst community structure, abundance and morphology in the Baltic Sea, Kattegat and Skagerrak. Estuar Coastal Shelf Sci. 155:1–7.
Stover LE, Evitt WR. 1978. Analyses of pre-Pleistocene organic-walled dinoflagellates. Stanford University Publications, Geological Sciences, v.15, 300 pp.
Van Nieuwenhove N, Bauch HA, Matthiessen J. 2008. Last interglacial surface water conditions in the eastern Nordic Seas inferred from dinocyst and foraminiferal assemblages. Marine Micropaleontol. 66(3–4):247–263.
Wall D, Dale B. 1968. Modern dinoflagellate cysts and the evolution of the Peridiniales. Marine Micropalaeontol. 14(3):265–304.
Williams GL, Stover LE, Kidson EJ. 1993. Morphology and stratigraphic ranges of selected Mesozoic-Cenozoic dinoflagellate taxa in the Northern Hemisphere. Geological Survey of Canada paper 92–10, 137 pp.
Zonneveld KAF, Marret F, Versteegh GJM, Bogus K, Bonnet S, Bouimetarhan I, Crouch E, de Vernal A, Elshanawany R, Edwards L, et al. 2013. Atlas of modern dinoflagellate cyst distribution based on 2405 data points. Rev Palaeobot Palynol. 191:1–97.